

Entropy of thermal quasiparticles in nuclei

M. Guttormsen*, M. Hjorth-Jensen, E. Melby, J. Rekstad, A. Schiller and S. Siem
Department of Physics, University of Oslo, P.O.Box 1048 Blindern, N-0316 Oslo, Norway

Information on level density for nuclei with mass numbers $A \sim 20$ –250 is deduced from discrete low-lying levels and neutron resonance data. The odd-mass nuclei exhibit in general 4 – 7 times the level density found for its neighboring even-even nuclei at the same excitation energy. This excess corresponds to an entropy of $\sim 1.7 k_B$ for the odd particle. The value is approximately constant for all mid-shell nuclei and for all ground state spins. For these nuclei it is argued that the entropy scales with the number of quasiparticles. A simple model based on the canonical ensemble theory accounts qualitatively for the observed properties.

PACS number(s): 21.10.Ma, 24.10.Pa, 65.50.+m, 64.60.Fr

I. INTRODUCTION

Nuclear structure at low excitation energy depends on the residual long-range two-body interaction. One of the most exciting consequences of this interaction is the forming of $J = 0$ nucleon pairs, the so-called Cooper pairs, where nucleons are moving in time reversed orbitals. It has been a great challenge to observe the breaking of these Cooper pairs and the general quenching of pair correlations as function of temperature T and angular frequency ω . Rotational high spin states are essentially described by quasiparticles coupled to the rotating underlying core. Backbending phenomena and spin alignments have been described according to their quasiparticle properties.

The concept of thermal quasiparticles is based on the idea that thermal properties at low excitation energy are governed by a few quasiparticles coupled to the cold core of Cooper pairs. These quasiparticles are thermally scattered on available single particle states. Thus, they are not well-defined by one single (Nilsson) orbital with given spin and parity, but exhibit an average of the spectroscopical properties of the orbitals in the vicinity of the Fermi surface. At higher temperatures ($T > 0.5$ MeV), the pair correlations are quenched and the core of Cooper pairs is no longer well defined [1].

The entropy is a fundamental quantity in the description of many body systems. For hot nuclei the entropy has the same importance as the spin alignment has for rotational nuclei. It can be evaluated from mechanical variables like energy, particle number and volume. Thus, it can be deduced in the microcanonical ensemble, which is the appropriate ensemble for an isolated system like the nucleus. The microcanonical entropy is defined for all isolated systems, from few-body systems up to infinite systems. It has been shown that phase transitions in small systems can be studied using the microcanonical entropy without invoking the thermodynamical limit [2].

Although less appropriate, also the canonical ensemble theory is widely applied to nuclei. One advantage of the canonical ensemble is that the thermodynamical observables are smooth functions of temperature due to the Laplace transformation involved in the calculation of the canonical partition function. Therefore, we will model our findings in this work within the canonical ensemble theory.

In a recent paper [3], we extracted the microcanonical single quasiparticle entropy in hot $^{161,162}\text{Dy}$ and $^{171,172}\text{Yb}$ nuclei to be 1.70(15) in units of the Boltzmann constant k_B . Furthermore, the single quasiparticle entropy was found to be approximately constant in the 1–6 MeV excitation region.

In this paper we will investigate the global systematics of nuclear entropy as function of nuclear mass, excitation energy (or temperature), number of excited quasiparticles and ground state spin. In Sect. II we sketch a simple model for thermal quasiparticles in nuclei. The method of determining level density by counting levels and using neutron resonance spacings is described in Sect. III. In Sect. IV we display the systematics of entropies and in Sect. V the properties of thermal quasiparticles are discussed. In Sect. VI we present an application involving thermal quasiparticles and, finally, concluding remarks are given in Sect. VII.

II. SIMPLE MODEL FOR THERMAL QUASIPARTICLES

In this section we will describe a simple model demonstrating the properties of thermal quasiparticles, which in turn will be compared to experimental data. The main task is to describe the partition function Z in the canonical ensemble for a given temperature T and number of thermal quasiparticles n . The thermodynamical quantities of interest can be deduced from the Helmholtz free

*Electronic address: magne.guttormsen@fys.uio.no

energy

$$F(T) = -T \ln Z(T), \quad (1)$$

where we express the temperature T in units of MeV and k_B is set to unity. From this bridge equation connecting statistical mechanics and thermodynamics, we may calculate the entropy S , the average excitation energy $\langle E \rangle$, the heat capacity C_V , and the chemical potential μ at the temperature T by

$$S(T) = - \left(\frac{\partial F}{\partial T} \right)_V \quad (2)$$

$$\langle E(T) \rangle = F + TS \quad (3)$$

$$C_V(T) = \left(\frac{\partial \langle E \rangle}{\partial T} \right)_V \quad (4)$$

$$\mu(T) = \frac{\partial F}{\partial n}, \quad (5)$$

where n is the number of thermal quasiparticles.

In the evaluation of the partition function Z , we assume spin 1/2 fermions scattered into a doubly degenerated single particle level scheme with equal energy spacing ϵ . The level scheme has infinitely many levels, and it is one scheme for protons and one for neutrons, as indicated in Fig. 1. These conditions simulate the Nilsson single particle scheme for deformed nuclei.

We will first construct the partition functions z_n^\uparrow for n identical spin-up fermions placed in one and the same single particle scheme. We assume that n quasiparticles are available, with the core of Cooper pairs as a reservoir. The total partition functions can then be expressed by these basic partition functions. The scattering of one spin-up fermion into the level scheme gives the partition function

$$z_1^\uparrow = \sum_{i=0}^{\infty} \exp(-i\epsilon/T) = \frac{1}{1 - \exp(-\epsilon/T)}. \quad (6)$$

When two identical spin-up fermions are placed into the same level scheme, the summing is restricted due to the Pauli principle by

$$\begin{aligned} z_2^\uparrow &= \sum_{i=0}^{\infty} \left[\exp(-i\epsilon/T) \sum_{j=i+1}^{\infty} \exp(-j\epsilon/T) \right] \\ &= \frac{1}{1 - \exp(-2\epsilon/T)} \frac{\exp(-\epsilon/T)}{1 - \exp(-\epsilon/T)} \\ &= z_1^\uparrow \frac{\exp(-\epsilon/T)}{1 - \exp(-2\epsilon/T)}. \end{aligned} \quad (7)$$

Generally, for n identical spin-up fermions we find

$$z_n^\uparrow = z_{n-1}^\uparrow \frac{\exp(-(n-1)\epsilon/T)}{1 - \exp(-n\epsilon/T)}. \quad (8)$$

We now allow spin up *and* down for the fermions, and evaluate the corresponding partition function z_n . For

one fermion with spin up *or* down we simply obtain a degeneration of two, since $z_1^\uparrow = z_1^\downarrow$:

$$z_1 = z_1^\uparrow + z_1^\downarrow = 2z_1^\uparrow. \quad (9)$$

If two fermions occupy the same level scheme, the partition function becomes more complicated. With the spins of the two fermions antiparallel ($m = m_1 + m_2 = 0$), no Pauli blocking is present and we obtain

$$z_2(m=0) = z_1^\uparrow z_1^\downarrow = \left(z_1^\uparrow \right)^2. \quad (10)$$

The contribution with parallel spin invoke the Pauli principle giving

$$z_2(m=\pm 1) = z_2^\uparrow + z_2^\downarrow = 2z_2^\uparrow. \quad (11)$$

It is now straightforward to evaluate z_n for n fermions, allowing spin up and down. For convenience we list the seven lowest partition functions here:

$$\begin{aligned} z_1 &= 2z_1^\uparrow \\ z_2 &= 2z_2^\uparrow + \left(z_1^\uparrow \right)^2 \\ z_3 &= 2z_3^\uparrow + 2z_2^\uparrow z_1^\uparrow \\ z_4 &= 2z_4^\uparrow + 2z_3^\uparrow z_1^\uparrow + \left(z_2^\uparrow \right)^2 \\ z_5 &= 2z_5^\uparrow + 2z_4^\uparrow z_1^\uparrow + 2z_3^\uparrow z_2^\uparrow \\ z_6 &= 2z_6^\uparrow + 2z_5^\uparrow z_1^\uparrow + 2z_4^\uparrow z_2^\uparrow + \left(z_3^\uparrow \right)^2 \\ z_7 &= 2z_7^\uparrow + 2z_6^\uparrow z_1^\uparrow + 2z_5^\uparrow z_2^\uparrow + 2z_4^\uparrow z_3^\uparrow. \end{aligned} \quad (12)$$

The partition function for nuclei with protons and neutrons may now be constructed from the partition functions z_n . In Fig. 1 the relevant configurations for the lowest quasiparticle excitations in the proton-odd system are illustrated. For this one-quasiparticle system, there is only one proton partition function to consider. For the three-quasiparticle case the $\pi\nu^2$ and the π^3 partition functions have to be included. For the two-quasiparticle case of the even-even system we assume that either a π or ν pair can be broken. In the four-quasiparticle case there are $\pi^2\nu^2$, π^4 and ν^4 configurations to take into account. From similar arguments for higher number of quasiparticles, we construct the seven lowest partition functions for proton-odd and even-even systems by

$$\begin{aligned} Z_1 &= z_1 \\ Z_2 &= 2z_2 \\ Z_3 &= z_3 + z_1 z_2 \\ Z_4 &= 2z_4 + (z_2)^2 \\ Z_5 &= z_5 + z_3 z_2 + z_1 z_4 \\ Z_6 &= 2z_6 + 2z_4 z_2 \\ Z_7 &= z_7 + z_5 z_2 + z_3 z_4 + z_1 z_6. \end{aligned} \quad (13)$$

The partition functions for the neutron-odd system are identical to the functions for the proton-odd system.

The partition functions for the odd-odd system can be constructed in a similar manner. The two-quasiparticle partition function is simply $(z_1)^2$, giving an entropy of twice the single quasiparticle entropy of the odd-mass system. Higher numbers of quasiparticles yield the following partition functions for the odd-odd case:

$$\begin{aligned}\tilde{Z}_2 &= (z_1)^2 \\ \tilde{Z}_4 &= 2z_3z_1 \\ \tilde{Z}_6 &= 2z_5z_1 + (z_3)^2 \\ \tilde{Z}_8 &= 2z_7z_1 + 2z_5z_3.\end{aligned}\quad (14)$$

The single quasiparticle entropy is easily computed from our model with Eqs. (1,2,13) as

$$S_1(T) = \frac{\epsilon/T}{\exp(\epsilon/T) - 1} + \ln \frac{2}{1 - \exp(-\epsilon/T)}. \quad (15)$$

At higher excitation energies more quasiparticles have to be considered and the mathematical expressions become more complicated. In Fig. 2 the calculated n -quasiparticle entropy S_n is shown as function of ϵ/T . The entropy is seen to scale rather well with the number of quasiparticles, and there is a weak Pauli-blocking effect. The reason for this apparent extensivity is the onset of new degrees of freedom with increasing number of quasiparticles. In our formalism, this is manifested in the additional terms in the partition function appearing from the inclusion of spin up/down quasiparticles and the breaking of proton/neutron pairs.

This approximate extensivity of the entropy can be utilized to estimate the many quasiparticle partition function as a simple product of n quasiparticle partition functions $Z_n = (Z_1)^n$. The quasiparticle entropy is then roughly given by

$$S_n = nS_1, \quad (16)$$

where we argue in Sect. IV that the S_1 value is experimentally available for most nuclei.

To create quasiparticles costs energy. In order to break one Cooper pair of the core the energy 2Δ is necessary. Taking this energy into account we can finally write the partition functions of even-even (ee), odd (odd) and odd-odd (oo) nuclei as weighted sums of the n -quasiparticle partition functions:

$$\begin{aligned}Z^{ee} &= 1 + e^{-2\Delta/T} Z_2 + e^{-4\Delta/T} Z_4 + \dots \\ Z^{\text{odd}} &= Z_1 + e^{-2\Delta/T} Z_3 + e^{-4\Delta/T} Z_5 + \dots \\ Z^{\text{oo}} &= \tilde{Z}_2 + e^{-2\Delta/T} \tilde{Z}_4 + e^{-4\Delta/T} \tilde{Z}_6 + \dots\end{aligned}\quad (17)$$

provided an ideal core of Cooper pairs, not changing with the number of quasiparticles. If the system is extensive, we may write the partition functions in closed form. By using the property of extensivity, $Z_n = (Z_1)^n$, and performing the sum up to N broken Cooper pairs¹, we obtain

$$\begin{aligned}Z^{ee} &= \frac{1 - (e^{-\Delta/T} Z_1)^{2N+2}}{1 - (e^{-\Delta/T} Z_1)^2} \\ Z^{\text{odd}} &= Z_1 Z^{ee} \\ Z^{\text{oo}} &= (Z_1)^2 Z^{ee}.\end{aligned}\quad (18)$$

The latter partition functions are good approximations for the expressions of Eq. (17) for up to ~ 2 broken pairs, however, for more than ~ 4 quasiparticles, the Pauli blocking cannot be neglected.

Figure 3 shows the entropy as function of temperature calculated from our model, allowing up to 5 broken nucleon pairs. Also calculations assuming extensivity of the entropy, in the sense $Z_n = (Z_1)^n$, are shown. There are serious discrepancies between the non-extensive and extensive approaches for $T > 0.3$ MeV.

There are limitations of the present model. The excited states are assumed built by a few quasiparticles, while the other particles are forming Cooper pairs in the underlying core. This picture will break down for (i) light nuclei, (ii) around closed shells and (iii) at high excitation energy. The first two points rest on the fact that the single particle energy spacing should be small or comparable to the pairing interaction in order to build a superfluid phase. The last point is connected to the thermal quenching of pair correlations, where many valence particles participate in the excitation. A fingerprint of the breakdown of the thermal quasiparticle picture is when the entropy in the odd-mass and even-even systems becomes essentially equal. These limitations have been addressed in Ref. [3].

III. DETERMINATION OF LEVEL DENSITY ANCHOR POINTS

The nuclear level density ρ is scarcely known as function of excitation energy. Recently [4], there has been published compilations of level density parameters. In our work we show that it is possible to determine two level density points quite reliably for numerous nuclei. To demonstrate the technique, Fig. 4 shows the two extracted anchor points (filled data points) for ¹⁷²Yb, together with the level density deduced from known discrete levels (solid lines). The first point (E_1, ρ_1) is based

¹For $N \rightarrow \infty$ broken Cooper pairs our simple model breaks down since the partition functions become infinite at the temperature $\epsilon/T = -\ln[1 - 2 \exp(-\Delta/T)]$.

on counting known discrete levels at low excitation energy, giving an anchor point in the excitation energy region of $0 < E < 2$ MeV. Information on known levels is taken from the database of Ref. [5], where we have analyzed levels of ~ 1600 nuclei. The second point (E_2, ρ_2) is estimated from the average neutron resonance spacing at the neutron binding energy B_n , where we use the compilation of Iljinov et al. [6].

Figure 4 also includes the data points [1] (open circles) obtained with the method of Ref. [7]. The dashed straight line describes the data rather well. This line will be referred to as the constant-temperature level-density formula, defined by

$$\rho(E) = Ce^{E/T} \quad (19)$$

with $T^{-1} = (\ln \rho_2 - \ln \rho_1)/(E_2 - E_1)$ and $C = \rho_1 \exp(-E_1/T)$. This line connecting the two anchor points is used to determine the nuclear temperature T .

In the extraction procedure of (E_1, ρ_1) , an initial slope is predicted for the straight line; in the case of ^{172}Yb , the inverse of $T = 0.57$ MeV. Then the two highest values of the count-based $\ln \rho$ relative to this line is found². With maximums at the energy bin numbers a and b , we find the lower anchor point by

$$\rho_1 = \exp \left[\frac{1}{b-a+1} \sum_{i=a}^b \ln \rho(i) \right] \quad (20)$$

with energy E_1 in bin number $(a+b)/2$. In the evaluation of the uncertainty of ρ_1 , the number of levels N ($\sigma_N = \sqrt{N}$) and the uncertainty of T ($\sigma_T = 0.1T$) are taken into account. Nuclei far from β -stability may have been poorly investigated due to low reaction cross sections, and the extracted level density and uncertainties of these nuclei should be adopted with caution.

The second point (E_2, ρ_2) is estimated from the average neutron resonance spacing at B_n . Assuming neutron $\ell = 0$ capture on a nucleus with target spin and parity I^π , levels with the same parity and two spins $I \pm 1/2$ are populated. In order to transfer the spacing \overline{D} between these levels to the level density for all spins and parities, we use the spin distribution of Gilbert and Cameron [8]

$$\rho_2 = \frac{2\sigma^2}{\overline{D}} \left[(I+1)e^{\frac{-(I+1)^2}{2\sigma^2}} + Ie^{\frac{-I^2}{2\sigma^2}} \right]^{-1}. \quad (21)$$

The spin cut-off parameter σ is defined through $\sigma^2 = 0.0888A^{2/3}\sqrt{aU}$, where the back-shifted energy is $U = E - E_{bs}$. The level density parameter a and the back-shift parameter E_{bs} are defined by $a = 0.21A^{0.87}$ MeV⁻¹ and $E_{bs} = C_{bs} + \Delta$, respectively, where the back-shift correction is given by $C_{bs} = -6.6A^{-0.32}$ according to Ref. [9].

²We pick the highest values since it is more probable that levels have escaped detection than the opposite.

The pairing gap parameter is estimated by $\Delta = 12A^{-1/2}$ MeV.

In Figs. 5-7 we show the anchor points extracted for nine isotopes of germanium, gadolinium and uranium, respectively. The above procedure has been tested carefully and found reliable, as demonstrated in these figures. In Table 1 the two anchor points are listed together with the temperature T for the nuclei where both anchor points are known. We also see from Table 1 and Figs. 5-7 that the extracted value of T is approximately equal for neighboring nuclei, thus, giving confidence to the methods applied for establishing the two anchor points.

IV. EXTRACTION OF ENTROPY

The measured level density $\rho(E)$ is proportional to the number of states accessible to the nuclear system at excitation energy E . Thus, the entropy in the microcanonical ensemble is given by

$$S(E) = \ln(\rho(E)/\rho_0) = \ln \rho(E) + S_0. \quad (22)$$

Applied to Eq. (19), parameter T is interpreted as the thermodynamical temperature in the microcanonical ensemble, since by definition:

$$\langle T(E) \rangle = \frac{1}{(\partial S / \partial E)_V}. \quad (23)$$

The constant shift parameter $S_0 = -\ln \rho_0$ can be adjusted to fulfill the third law of thermodynamics; $S \rightarrow 0$ when $T \rightarrow 0$. The condition $T = 0$ probably holds for the rotational ground band of deformed even-even nuclei. However, also other interpretations for $T = 0$ are possible, and we will not fix the S_0 parameter to a specific value in this work, but instead discuss the relative entropy $S - S_0 = \ln \rho$.

The level density in between the two anchor points is not very well known. Recently [1,10], the level densities for $^{161,162}\text{Dy}$, ^{166}Er and $^{171,172}\text{Yb}$ have been measured. A common feature for these nuclei, is that the level densities develop more like the constant temperature level density formula of Eq. (19), than the back-shifted Fermi-gas level density [9], as pointed out in the discussion of Fig. 4 and Ref. [11]. This constant temperature behavior is interpreted [1,10] as the breaking of Cooper pairs with increasing excitation energy.

In the following, we will discuss the microcanonical entropy for given excitation energy E . In order to establish a common play ground, we extrapolate the first and second level density anchor points to excitation energies 1 and 7 MeV, using the constant temperature formula of

Eq. (19). Figures 8 and 9 display the entropy $S - S_0$ based on the two anchor points evaluated at 1 and 7 MeV, respectively. The data are plotted as function of the mass number, where nuclei along the β -stability line are chosen.

V. THERMAL QUASIPARTICLE PROPERTIES

A. Regions of quasiparticle extensivity

In the lower panel of figure 8 the difference in entropy between odd-mass and even-even systems $\Delta S = S_{\text{odd}} - S_{\text{ee}}$ is shown. The data show fluctuations which are partly due to shell closures, incomplete knowledge of discrete levels at low excitation energy, and structural changes between various isotopes and isotones. For the mid-shell regions the odd-mass nuclei have about $\Delta S \sim 1.7$ higher entropy compared to the even-even system. This feature holds for odd-even as well as for even-odd nuclei, however, neutrons carries slightly more entropy than protons. In Fig. 9 the data are sensitive to the level density extracted from neutron resonance level spacing. The fluctuations are less pronounced at 7 MeV because the level density is based on many quasiparticle states, smearing out structural effects. Also here, as indicated on the figure by lines, an entropy difference of $\Delta S \sim 1.7$ is found. Here, we should remember that these findings are based on a constant temperature level density extrapolation. If a Fermi gas level density is applied, e.g. the model of Egidy et al. shown in Fig. 4, the extracted microcanonical entropy difference ΔS will be somewhat modified; it will increase at 1 MeV and decrease at 7 MeV. However, as demonstrated in Ref. [3], the experimental value of ΔS is rather constant for excitation energies above 1.5 MeV.

It is amazing that ΔS is roughly the same both at 1 and 7 MeV of excitation energy. This means that even with 4 – 6 quasiparticles excited at 7 MeV [3], the last thermal quasiparticle still carries $\Delta S \sim 1.7$. Thus, the experimental entropy scales with the number of quasiparticles. This property is also accounted for in our model³. The regions of quasiparticle extensivity can be identified in Figs. 8 and 9 as entropy-gaps between the entropies of odd-mass and even-even nuclei. The extensivity regions are found for mid-shell nuclei with mass number $A > 40$.

In odd-odd nuclei, several neutron energy spacing data are known [6]. As seen in Fig. 9 (see lines), a proton and a neutron give an entropy excess of around $2\Delta S \sim 3.4$, as expected from the discussion in Sect. II. A similar

study from known discrete levels is difficult, due to experimental limitations in building level schemes with several hundreds of levels per MeV. However, in the case of the well studied odd-odd ^{152,154}Eu isotopes the lower anchor point seems to have been determined with acceptable confidence. Figure 10 shows that an additional neutron outside the odd-proton core gives an entropy difference as high as 2.5. The extracted temperatures are all lying within a narrow window of $T = 0.57 - 0.60$ MeV.

The feature that ΔS is approximately independent of excitation energy E is shown in Table 1. Here, constant temperature T for neighboring mid-shell nuclei means that the slope of $\ln \rho$ is equal and, thus, ΔS is approximately independent of E . Fig. 11 confirms the systematics, where neighboring nuclei exhibit the same $(\partial S / \partial E)$ value. This indicates that the level density, and hence the entropy, has the same functional form as function of excitation energy. However, the feature disappears at shell closures.

B. Constancy of quasiparticle entropy

Figure 12 shows the entropy difference for a neutron outside its even-even core for various rare earth elements. Although various mid-shell isotopes reveal quasiparticle entropy that deviates from $\Delta S \sim 1.7$ it is still surprising how constant this quantity appears to be. However, as shown in Fig. 12, the quasiparticle around the $N = 82$ shell closure carries low entropy due to the limited number of quantum states (multiplicity) available for the system.

Our model gives a qualitative interpretation of the constancy of the quasiparticle entropy. With the assumptions given, the model shows that the entropy S_n is a function of ϵ/T , only. In order to deduce experimentally the value of ϵ/T , we recognize that the single particle level spacing ϵ is connected to the level density parameter a by [12]

$$a = \frac{\pi^2}{6}(g_p + g_n) \sim \frac{\pi^2}{3}g = \frac{\pi^2}{3\epsilon}, \quad (24)$$

where the single-particle level-density parameters for protons and neutrons (g_p and g_n) are assumed to be approximately equal. Thus, we obtain using Eq. (23)

$$\frac{\epsilon}{T} = \frac{\pi^2}{3a} \left(\frac{\partial S}{\partial E} \right). \quad (25)$$

In Fig. 13 the quantity $(\partial S / \partial E) / a$ is plotted as function of mass number A , using the a values of Ref. [6] and the data of Fig. 11. For increasing A , the extracted values

³We should keep in mind that the model is formulated in the canonical ensemble, where a certain temperature T corresponds to a wide excitation energy range.

are found in the range of 0.10 – 0.08, which corresponds to $\epsilon/T = 0.33 - 0.26$ according to Eq. (25). This variation gives a minor effect on the predicted single particle entropy S_1 ; Fig. 2 shows that the variation in ϵ/T corresponds to an increase of S_1 from 2.7 to 3.0.

The experimentally extracted single quasiparticle entropy ΔS shows no clear systematic trend as function of A within the uncertainties. Essentially, the local variations due to structural changes between neighboring nuclei are more pronounced than the weak variation in S_1 given by the model.

The quasiparticle entropy ΔS could in principle depend on the odd-mass ground state spin, since an orbital with high spin has more coupling combinations to the underlying rotating core. For excitation energies around the neutron binding energy B_n , the ground state orbital participates no more than other orbitals around the Fermi level, so no resemblance of the ground state spin is expected. However, around the lower anchor point (E_1, ρ_1) , the ground state orbital could play a role. In Fig. 14 we see no significant effect for rare earth nuclei, and the same result applies to other mass regions. This indicates that many orbitals participate to build up the level density in the lower excitation region of odd-mass nuclei.

To close this subsection, we point out that Fig. 14 indicates an average quasiparticle entropy ΔS of ~ 1.5 and ~ 1.9 for protons and neutrons, respectively. The valence protons and neutrons in this figure occupy orbitals in the $Z = 50 - 82$ and $N = 82 - 126$ shells, containing 32 and 44 orbitals, respectively. Thus, the single particle level energy spacing is expected to scale roughly as $\epsilon_p/\epsilon_n = 44/32 \sim 1.4$. According to Fig. 2, a 40% variation in ϵ/T around the value $\epsilon/T = 0.3$ gives a change in S_1 of about 0.4. Therefore, this effect could be the reason why the protons carry slightly less entropy compared to the neutrons.

VI. APPLICATION OF THERMAL QUASIPARTICLES

There are several applications for the concepts presented here. In analogy with the description of rotational nuclei [13], the Helmholtz free energy F plays the same role as the energy in the rotating frame E' . To visualize the analogy, the two cases read

$$F = E - TS \quad (26)$$

$$E' = E - \omega I_x, \quad (27)$$

where ω is the rotational frequency and I_x is the spin alignment along the rotational x-axis. Generally, S and I_x are positive quantities, so that F and E' decreases

with increasing T and ω , respectively. A decoupled Cooper pair with high I_x may, at a certain critical frequency ω_c , become more favoured than its coupled counterpart, giving rise to the rotational backbending phenomenon.

In a similar manner, we will here demonstrate that the free energy of a system with two additional excited quasiparticles becomes favoured at a critical temperature T_c . This temperature depends on the pairing gap Δ and the quasiparticle entropy ΔS . If both these quantities would be independent of the number of quasiparticles excited, a break-up of all Cooper pairs should happen at one and the same critical temperature T_c , giving rise to a strong quenching of the pair correlations.

Let us assume that the partition function for an even-even nucleus is described by $Z(T) = Z_{\text{core}}(T)$. This partition function represents the lowest free energy $F(T)$ at low temperatures T . We now introduce the breaking of one pair relative to this core⁴. Assuming the two quasiparticles to be independent of the core, we may describe the excited system by a factorization of the partition function into

$$Z^* \approx Z_{\text{core}} Z_2 e^{-2\Delta/T}, \quad (28)$$

where Z_2 is the two quasiparticle partition function. With this assumption, the difference in Helmholtz free energy becomes

$$\Delta F = -T(\ln Z^* - \ln Z_{\text{core}}) = -T \ln Z_2 + 2\Delta, \quad (29)$$

and factorizing Z_2 assuming extensivity, gives

$$\Delta F = -T \ln Z_1^2 + 2\Delta = 2(F_1 + \Delta), \quad (30)$$

where F_1 is the free energy of one quasiparticle. This corresponds to the chemical potential defined (see Eq. (5)) as the energy required to bring one quasiparticle out of the reservoir:

$$\mu(T) = \Delta F/2 = F_1 + \Delta. \quad (31)$$

We have applied this formalism to the experimental data of $^{161,162}\text{Dy}$, see Ref. [3]. The partition functions for each nucleus are calculated by

$$Z(T) = \sum_E \Delta E \rho(E) e^{-E/T} \quad (32)$$

where ΔE is the experimental energy bin. The assumptions made for evaluating Z is given elsewhere [3]. The corresponding Helmholtz free energy F for ^{162}Dy is displayed in the upper panel of Fig. 15. The upper energy curve, based on data for ^{161}Dy , is given by $F(^{161}\text{Dy}) +$

⁴The core described by Z_{core} is not necessary a cold core, but may already have pairs broken.

Δ_n , where the pairing gap parameter is determined from neutron separation energies \mathcal{S}_n by

$$\Delta_n = \frac{1}{4} |\mathcal{S}_n(N+1, Z) - 2\mathcal{S}_n(N, Z) + \mathcal{S}_n(N-1, Z)|, \quad (33)$$

giving $\Delta_n = 0.917$ MeV for ^{162}Dy . Thus, the energy curve of ^{161}Dy can be interpreted as the free energy for an even-even system with one extra quasiparticle. We therefore identify $F_1 + \Delta_n$ in Eq. (30) with the difference $F(^{161}\text{Dy}) + \Delta_n - F(^{162}\text{Dy})$.

In the lower panel of Fig. 15 the chemical potential $\mu = F_1 + \Delta_n$ is shown as function of temperature. The higher entropy in ^{161}Dy compared to ^{162}Dy decreases the free energy relative to the even-even core with increasing temperature. When $\mu(T) \sim 0$, thermal quasiparticles can be formed without consuming free energy. Thus, from Fig. 15 we estimate the critical temperature⁵ for the quenching of pair correlations to be $T_c = 0.42$ MeV. The uncertainty of this number is mainly due to the extensivity assumed in the evaluation of ΔF . Furthermore, the adoption of a chemical potential $\mu = \Delta$ at $T = 0$, rests on the assumption that the Fermi level coincides with single particle energies in both nuclei. Also the extrapolation of the experimental level density to higher excitation energies, see Ref. [1], gives systematical errors. From these considerations we estimate a 15 % error in the T_c value.

The deduced value of $T_c = 0.42(6)$ is considered to be common to the two dysprosium isotopes analyzed. Recently [1], values of $T_c = 0.52(4)$ and $0.49(4)$ MeV were found for ^{161}Dy and ^{162}Dy , respectively, using the canonical heat capacity as thermometer for the phase transition.

Finally, we point out a curious connection between the experimental quasiparticle entropy ΔS and the critical temperature T_c deduced from a Fermi gas model with pairing. If we assume a constant ΔS and a constant differences Δ between the E functions for the two curves of Fig. 15, we find

$$T_c = \frac{1}{\Delta S} \Delta, \quad (34)$$

giving $T_c = 0.59\Delta$ for $\Delta S = 1.7$. This estimate coincides almost exactly with the theoretical expression $T_c = 0.57\Delta$ given in Refs. [14,15]. The theoretical factor 0.57 is independent on the mass number, consistent with the property of the experimental single quasiparticle entropy.

⁵At the critical temperature T_c we have $F_1 = -\Delta = -T_c \ln Z_1$, and applying $Z_1 = 2z_1^\uparrow$, we get $\epsilon/T_c = -\ln[1 - 2 \exp(-\Delta/T_c)]$, the same expression as in footnote 1.

VII. CONCLUSIONS

We have analyzed the level densities of nuclei based on counting discrete levels and from neutron scattering data. It was possible to obtain level density anchor points for about 280 nuclei. The level densities have been transformed into microcanonical entropy, revealing the phase space of the system at fixed excitation energies.

The single quasiparticle entropy has been extracted from the odd-even entropy differences. The quasiparticles not coupled in Cooper pairs, exhibit an entropy of $\Delta S \sim 1.7$ which is relatively independent of the presence of other quasiparticles. This apparent extensivity is valid for mid-shell nuclei and for all ground state spins. A simple model for thermal quasiparticles in the canonical ensemble also supports the property of extensivity.

The single quasiparticle entropy ΔS for mid-shell nuclei shows no clear mass dependency. This is explained in our model by the fact that ΔS only depends on the ratio between the single particle spacing ϵ and the temperature T , which is found to be almost independent of the mass number for mid-shell nuclei.

For thermal systems, the Helmholtz free energy is analogous to the energy in the internal frame of rotating nuclei. This opens for the study of various quantities and critical phenomena as function of temperature. We therefore believe that the concept of single quasiparticle entropy may provide a fruitful basis for the understanding of hot nuclei.

The simple model presented here is only adequate for mid-shell nuclei. Around closed shells one expects exciting effects from the increasing single particle energy spacings. This will also influence the entropy difference between odd-mass and even-even nuclei. Therefore, a statistical description of the transition to closed shells would be of great interest.

We wish to acknowledge the support from the Norwegian Research Council (NFR).

-
- [1] A. Schiller, A. Bjerve, M. Guttormsen, M. Hjorth-Jensen, F. Ingebretsen, E. Melby, S. Messelt, J. Rekestad, S. Siem, and S.W. Ødegård, preprint nucl-ex/9909011.
 - [2] D.H.E. Gross and E. Votyakov, Eur. Phys. **15**, 117 (2000).
 - [3] M. Guttormsen, A. Bjerve, M. Hjorth-Jensen, E. Melby, J. Rekestad, A. Schiller, S. Siem, and A. Belic, Phys. Rev. **C62**, 024306 (2000).

- [4] Handbook for calculations of nuclear reaction data, IAEA, Vienna, IAEA-TECDOC-1024 (1998) p. 11 and 69.
- [5] Data extracted using the NNDC On-Line Data Service from the ENSDF database, file revised as of Jan. 21, 2000.
- [6] A.S. Iljinov, M.V. Mebel, N. Bianchi, E. De Sanctis, C. Guaraldo, V. Lucherini, V. Muccifora, E. Polli, A.R. Reolon, and P. Rossi, Nucl. Phys. **A543**, 517 (1992).
- [7] A. Schiller, L. Bergholt, M. Guttormsen, E. Melby, J. Rekstad, and S. Siem, Nucl. Instrum. Methods **A447**, 494 (2000).
- [8] A. Gilbert and A.G.W. Cameron, Can. J. Phys. **43**, 1446 (1965).
- [9] T. von Egidy, H.H. Schmidt and A.N. Behkami, Nucl. Phys. **A481**, 189 (1988).
- [10] E. Melby, L. Bergholt, M. Guttormsen, M. Hjorth-Jensen, F. Ingelbretsen, S. Messelt, J. Rekstad, A. Schiller, S. Siem and S.W. Ødegård, Phys. Rev. Lett. **83**, 3150 (1999).
- [11] M. Guttormsen, M. Hjorth-Jensen, E. Melby, J. Rekstad, A. Schiller, and S. Siem, Phys. Rev. **C61**, 067302 (2000).
- [12] A. Bohr and B. Mottelson, *Nuclear Structure*, (Benjamin, New York, 1969), Vol. I, p. 169.
- [13] R. Bengtsson and S. Frauendorf, Nucl. Phys. **A327**, 137 (1979).
- [14] M. Sano and S. Yamasaki, Prog. Theor. Phys. **29**, 397 (1963).
- [15] A.V. Ignatyuk et al., Yad. Fiz. **29** (1979) 875 [Sov. J. Nucl. Phys. **29** (1979) 450].

Table 1: Level density anchor points and temperatures.

Nuclide	E_1 (MeV)	ρ_1 (MeV ⁻¹)	E_2 (MeV)	ρ_2 (MeV ⁻¹)	T (MeV)
²⁰ F	2.70	6(2)	6.60	0.27E+02(0.70E+01)	2.53(63)
²⁴ Na	1.62	6(3)	6.96	0.38E+02(0.12E+02)	3.04(90)
²⁵ Mg	0.78	3(2)	7.33	0.18E+02(0.57E+01)	3.4(14)
²⁶ Mg	4.92	12(7)	11.09	0.76E+02(0.24E+02)	3.3(12)
²⁸ Al	1.32	5(2)	7.73	0.77E+02(0.21E+02)	2.29(43)
²⁹ Si	2.22	4(3)	8.47	0.54E+02(0.17E+02)	2.40(71)
³² P	3.36	9(2)	7.94	0.91E+02(0.37E+02)	2.00(43)
³³ S	2.46	5(2)	8.64	0.82E+02(0.21E+02)	2.20(41)
³⁴ S	2.70	4(3)	11.42	0.16E+03(0.62E+02)	2.34(51)
³⁵ S	3.06	7(2)	6.99	0.60E+02(0.22E+02)	1.84(44)
³⁶ Cl	3.24	12(2)	8.58	0.37E+03(0.12E+03)	1.56(17)
³⁸ Cl	1.86	10(5)	6.11	0.22E+03(0.69E+02)	1.39(26)
⁴¹ Ar	0.36	3(2)	6.10	0.14E+03(0.37E+02)	1.52(31)
⁴⁰ K	2.58	21(6)	7.80	0.12E+04(0.16E+03)	1.30(10)
⁴¹ K	3.90	34(6)	10.10	0.26E+04(0.26E+03)	1.44(7)
⁴² K	1.44	37(12)	7.53	0.11E+04(0.28E+03)	1.81(23)
⁴¹ Ca	3.12	11(3)	8.36	0.34E+03(0.82E+02)	1.54(17)
⁴³ Ca	2.88	29(7)	7.93	0.56E+03(0.11E+03)	1.71(19)
⁴⁴ Ca	3.90	17(5)	11.13	0.21E+04(0.33E+03)	1.50(10)
⁴⁵ Ca	1.68	10(4)	7.42	0.48E+03(0.98E+02)	1.49(18)
⁴⁹ Ca	3.00	9(3)	5.15	0.57E+02(0.20E+02)	1.14(33)
⁴⁶ Sc	0.24	17(9)	8.76	0.43E+04(0.33E+03)	1.54(16)
⁴⁷ Ti	2.70	54(23)	8.88	0.11E+04(0.19E+03)	2.07(32)
⁴⁸ Ti	4.02	28(6)	11.63	0.32E+04(0.82E+03)	1.60(11)
⁴⁹ Ti	2.58	19(7)	8.14	0.91E+03(0.17E+03)	1.44(15)
⁵⁰ Ti	3.42	12(4)	10.94	0.16E+04(0.39E+03)	1.54(14)
⁵¹ Ti	1.92	6(2)	6.37	0.24E+03(0.14E+03)	1.23(23)
⁵¹ V	3.54	59(23)	11.05	0.86E+04(0.20E+04)	1.51(14)
⁵² V	1.32	9(3)	7.31	0.13E+04(0.16E+03)	1.22(8)
⁵¹ Cr	1.14	6(2)	9.26	0.13E+04(0.22E+03)	1.49(12)
⁵³ Cr	1.86	7(2)	7.94	0.67E+03(0.13E+03)	1.32(10)
⁵⁴ Cr	2.64	8(3)	9.72	0.11E+04(0.38E+03)	1.46(15)
⁵⁵ Cr	0.42	6(3)	6.25	0.30E+03(0.54E+02)	1.47(23)
⁵⁶ Mn	0.66	15(5)	7.27	0.20E+04(0.32E+03)	1.35(11)
⁵⁵ Fe	0.66	3(2)	9.30	0.11E+04(0.22E+03)	1.48(19)
⁵⁷ Fe	0.66	4(2)	7.65	0.83E+03(0.15E+03)	1.33(11)
⁵⁸ Fe	2.46	10(4)	10.05	0.19E+04(0.52E+03)	1.45(13)
⁵⁹ Fe	0.84	8(4)	6.58	0.57E+03(0.25E+03)	1.36(20)
⁶⁰ Co	1.08	19(3)	7.49	0.42E+04(0.61E+03)	1.19(5)
⁶¹ Co	1.44	12(4)	9.32	0.22E+05(0.16E+04)	1.06(5)
⁵⁹ Ni	1.02	6(2)	9.00	0.17E+04(0.29E+03)	1.40(8)
⁶⁰ Ni	3.84	30(8)	11.40	0.51E+04(0.12E+04)	1.47(10)
⁶¹ Ni	2.04	32(11)	7.82	0.14E+04(0.26E+03)	1.53(16)
⁶² Ni	3.66	27(6)	10.60	0.51E+04(0.84E+03)	1.32(7)
⁶³ Ni	1.14	9(5)	6.84	0.11E+04(0.24E+03)	1.18(13)
⁶⁵ Ni	0.48	4(3)	6.10	0.75E+03(0.17E+03)	1.05(15)
⁶⁴ Cu	1.68	49(7)	7.92	0.11E+05(0.14E+04)	1.16(4)
⁶⁶ Cu	0.30	13(6)	7.07	0.74E+04(0.16E+04)	1.07(8)
⁶⁵ Zn	0.96	25(10)	7.98	0.67E+04(0.20E+04)	1.26(11)
⁶⁷ Zn	1.86	31(7)	7.05	0.36E+04(0.66E+03)	1.09(6)
⁶⁸ Zn	3.42	37(8)	10.20	0.21E+05(0.26E+04)	1.07(4)
⁶⁹ Zn	1.20	18(6)	6.48	0.27E+04(0.46E+03)	1.06(8)
⁷¹ Zn	0.60	8(3)	5.83	0.33E+04(0.58E+03)	0.86(7)
⁷⁰ Ga	1.14	57(12)	7.65	0.35E+05(0.88E+04)	1.02(5)
⁷² Ga	0.54	44(7)	6.52	0.21E+05(0.43E+04)	0.97(4)
⁷¹ Ge	1.32	51(14)	7.42	0.13E+05(0.53E+04)	1.10(10)
⁷³ Ge	0.84	42(13)	6.78	0.12E+05(0.20E+04)	1.06(7)

⁷⁴ Ge	2.64	28(5)	10.20	0.74E+05(0.80E+04)	0.96(3)
⁷⁵ Ge	0.24	20(9)	6.51	0.66E+04(0.14E+04)	1.09(9)
⁷⁷ Ge	0.60	20(9)	6.07	0.32E+04(0.44E+03)	1.08(10)
⁷⁶ As	0.54	82(15)	7.33	0.89E+05(0.12E+05)	0.97(3)
⁷⁵ Se	1.08	62(16)	8.03	0.67E+05(0.39E+05)	1.00(9)
⁷⁷ Se	0.96	34(8)	7.42	0.36E+05(0.80E+04)	0.93(4)
⁷⁸ Se	2.52	29(7)	10.50	0.15E+06(0.30E+05)	0.94(4)
⁷⁹ Se	0.66	24(7)	6.96	0.16E+05(0.33E+04)	0.97(6)
⁸¹ Se	0.60	12(7)	6.70	0.81E+04(0.35E+04)	0.93(10)
⁸³ Se	0.48	17(8)	5.82	0.39E+04(0.73E+03)	0.98(10)
⁸⁰ Br	0.36	75(18)	7.89	0.17E+06(0.21E+05)	0.98(3)
⁸² Br	0.90	43(11)	7.59	0.98E+05(0.18E+05)	0.87(4)
⁷⁹ Kr	0.84	44(9)	8.36	0.13E+06(0.37E+05)	0.94(4)
⁸¹ Kr	0.96	41(14)	7.88	0.11E+06(0.12E+05)	0.88(4)
⁸³ Kr	0.84	11(3)	7.46	0.80E+05(0.51E+05)	0.75(6)
⁸⁶ Rb	1.08	32(11)	8.65	0.77E+05(0.16E+05)	0.97(5)
⁸⁸ Rb	0.30	12(7)	6.08	0.57E+04(0.16E+04)	0.94(10)
⁸⁵ Sr	1.14	16(4)	8.53	0.83E+05(0.32E+05)	0.86(5)
⁸⁷ Sr	1.50	9(4)	8.43	0.34E+05(0.11E+05)	0.85(6)
⁸⁸ Sr	2.52	16(9)	11.11	0.60E+05(0.67E+04)	1.04(7)
⁸⁹ Sr	2.04	20(9)	6.37	0.25E+04(0.49E+03)	0.90(9)
⁹⁰ Y	0.96	9(4)	6.86	0.15E+05(0.28E+04)	0.80(5)
⁹¹ Zr	2.28	37(15)	7.20	0.52E+04(0.10E+04)	1.00(9)
⁹² Zr	1.44	8(6)	8.64	0.24E+05(0.68E+04)	0.90(9)
⁹³ Zr	1.80	16(4)	6.73	0.13E+05(0.36E+04)	0.74(4)
⁹⁵ Zr	1.80	18(6)	6.46	0.13E+05(0.25E+04)	0.71(4)
⁹⁷ Zr	1.20	8(6)	5.58	0.11E+05(0.30E+04)	0.61(7)
⁹⁴ Nb	1.14	61(13)	7.23	0.98E+05(0.14E+05)	0.82(3)
⁹³ Mo	2.76	103(21)	8.07	0.20E+05(0.38E+04)	1.01(5)
⁹⁵ Mo	0.90	17(9)	7.37	0.30E+05(0.97E+04)	0.87(7)
⁹⁶ Mo	2.58	44(11)	9.15	0.86E+05(0.12E+05)	0.87(3)
⁹⁷ Mo	0.90	20(5)	6.82	0.35E+05(0.61E+04)	0.80(3)
⁹⁸ Mo	2.46	51(12)	8.64	0.99E+05(0.15E+05)	0.82(3)
⁹⁹ Mo	0.78	35(10)	5.93	0.34E+05(0.84E+04)	0.75(4)
¹⁰¹ Mo	0.42	44(11)	5.40	0.46E+05(0.56E+04)	0.72(3)
¹⁰⁰ Tc	0.42	75(14)	6.76	0.28E+06(0.55E+05)	0.77(3)
¹⁰⁰ Ru	2.34	46(9)	9.67	0.24E+06(0.53E+05)	0.86(3)
¹⁰² Ru	2.16	24(4)	9.22	0.46E+06(0.61E+05)	0.72(2)
¹⁰³ Ru	0.36	34(8)	6.23	0.64E+05(0.19E+05)	0.78(4)
¹⁰⁴ Ru	1.38	11(6)	8.91	0.11E+07(0.56E+06)	0.65(4)
¹⁰⁴ Rh	0.48	121(22)	7.00	0.56E+06(0.81E+05)	0.77(2)
¹⁰⁵ Pd	0.66	33(6)	7.09	0.16E+06(0.25E+05)	0.76(2)
¹⁰⁶ Pd	2.52	56(11)	9.56	0.65E+06(0.97E+05)	0.75(2)
¹⁰⁷ Pd	0.54	24(11)	6.54	0.14E+06(0.48E+05)	0.69(5)
¹⁰⁸ Pd	2.16	23(6)	9.22	0.72E+06(0.13E+06)	0.68(2)
¹⁰⁹ Pd	0.48	46(14)	6.15	0.19E+06(0.77E+05)	0.68(4)
¹¹¹ Pd	0.36	28(7)	5.75	0.10E+06(0.17E+05)	0.66(3)
¹⁰⁸ Ag	0.60	115(22)	7.27	0.70E+06(0.15E+06)	0.77(3)
¹¹⁰ Ag	0.48	87(19)	6.81	0.98E+06(0.20E+06)	0.68(2)
¹⁰⁷ Cd	0.66	14(4)	7.93	0.31E+06(0.85E+05)	0.73(3)
¹⁰⁹ Cd	0.96	26(7)	7.35	0.34E+06(0.91E+05)	0.67(3)
¹¹¹ Cd	0.84	38(9)	6.98	0.26E+06(0.42E+05)	0.70(2)
¹¹² Cd	2.88	190(57)	9.40	0.86E+06(0.16E+06)	0.77(3)
¹¹³ Cd	1.08	87(19)	6.54	0.20E+06(0.44E+05)	0.71(3)
¹¹⁴ Cd	1.86	19(10)	9.04	0.83E+06(0.13E+06)	0.67(3)
¹¹⁵ Cd	0.60	20(6)	6.14	0.17E+06(0.30E+05)	0.61(2)
¹¹⁷ Cd	0.24	24(10)	5.77	0.10E+06(0.25E+05)	0.66(4)
¹¹⁴ In	1.08	68(16)	7.28	0.10E+07(0.15E+06)	0.65(2)
¹¹⁶ In	0.90	80(15)	6.78	0.73E+06(0.52E+05)	0.65(1)
¹¹³ Sn	1.14	19(7)	7.75	0.28E+06(0.95E+05)	0.69(4)

¹¹⁵ Sn	0.60	12(7)	7.55	0.19E+06(0.68E+05)	0.72(5)
¹¹⁶ Sn	2.22	16(7)	9.56	0.54E+06(0.27E+06)	0.70(5)
¹¹⁷ Sn	1.56	44(17)	6.95	0.11E+06(0.40E+05)	0.69(5)
¹¹⁸ Sn	2.22	27(11)	9.33	0.53E+06(0.13E+06)	0.72(3)
¹¹⁹ Sn	1.08	18(6)	6.49	0.70E+05(0.19E+05)	0.66(3)
¹²⁰ Sn	1.74	12(4)	9.11	0.38E+06(0.83E+05)	0.71(3)
¹²¹ Sn	1.02	24(8)	6.17	0.42E+05(0.13E+05)	0.69(4)
¹²³ Sn	1.02	28(13)	5.95	0.26E+05(0.13E+05)	0.72(7)
¹²⁵ Sn	0.96	20(9)	5.73	0.17E+05(0.82E+04)	0.71(7)
¹²² Sb	0.24	62(16)	6.81	0.53E+06(0.72E+05)	0.73(2)
¹²⁴ Sb	0.48	61(16)	6.47	0.34E+06(0.41E+05)	0.69(2)
¹²³ Te	0.60	25(10)	6.93	0.32E+06(0.12E+06)	0.67(4)
¹²⁴ Te	2.76	112(22)	9.43	0.14E+07(0.34E+06)	0.71(2)
¹²⁵ Te	0.54	24(8)	6.57	0.20E+06(0.50E+05)	0.67(3)
¹²⁶ Te	2.28	46(10)	9.11	0.66E+06(0.83E+05)	0.71(2)
¹²⁷ Te	0.72	29(13)	6.29	0.74E+05(0.14E+05)	0.71(4)
¹²⁹ Te	0.60	16(5)	6.09	0.22E+05(0.70E+04)	0.75(5)
¹³¹ Te	0.96	25(10)	5.93	0.79E+04(0.13E+04)	0.86(7)
¹²⁸ I	0.30	75(14)	6.83	0.52E+06(0.14E+06)	0.74(3)
¹³⁰ I	0.24	47(14)	6.46	0.32E+06(0.62E+05)	0.71(3)
¹²⁵ Xe	0.72	45(9)	7.60	0.76E+06(0.83E+05)	0.71(2)
¹²⁹ Xe	0.42	24(8)	6.91	0.18E+06(0.21E+05)	0.73(3)
¹³⁰ Xe	2.64	58(15)	9.26	0.82E+06(0.11E+06)	0.69(2)
¹³¹ Xe	0.84	23(7)	6.62	0.25E+06(0.82E+05)	0.62(3)
¹³² Xe	2.16	29(11)	8.94	0.35E+06(0.13E+06)	0.72(4)
¹³³ Xe	0.96	20(9)	6.45	0.63E+05(0.65E+04)	0.68(4)
¹³⁶ Xe	2.52	29(11)	7.99	0.27E+05(0.60E+04)	0.80(5)
¹³⁴ Cs	0.42	62(10)	6.89	0.44E+06(0.54E+05)	0.73(2)
¹³⁵ Cs	0.36	8(6)	8.83	0.68E+06(0.13E+06)	0.75(5)
¹³⁷ Cs	1.26	9(3)	8.27	0.15E+06(0.32E+05)	0.72(3)
¹³¹ Ba	0.66	28(9)	7.49	0.76E+06(0.11E+06)	0.67(2)
¹³³ Ba	0.72	18(6)	7.19	0.37E+06(0.97E+05)	0.65(3)
¹³⁵ Ba	1.08	25(7)	6.97	0.13E+06(0.37E+05)	0.69(3)
¹³⁶ Ba	2.22	40(10)	9.11	0.41E+06(0.11E+06)	0.75(3)
¹³⁷ Ba	0.48	4(3)	6.90	0.55E+05(0.13E+05)	0.68(5)
¹³⁸ Ba	1.80	11(5)	8.61	0.71E+05(0.24E+05)	0.78(5)
¹³⁹ Ba	2.04	62(16)	4.72	0.31E+04(0.93E+03)	0.69(7)
¹³⁹ La	1.38	28(9)	8.78	0.42E+06(0.63E+05)	0.77(3)
¹⁴⁰ La	1.20	92(21)	5.16	0.35E+05(0.28E+04)	0.67(3)
¹³⁷ Ce	1.20	29(11)	7.48	0.52E+06(0.85E+05)	0.64(3)
¹⁴¹ Ce	2.10	47(11)	5.43	0.16E+05(0.54E+04)	0.57(4)
¹⁴² Pr	0.90	34(7)	5.84	0.16E+06(0.39E+05)	0.59(2)
¹⁴³ Nd	2.04	83(25)	6.12	0.75E+05(0.11E+05)	0.60(3)
¹⁴⁴ Nd	2.64	78(18)	7.82	0.24E+06(0.32E+05)	0.64(2)
¹⁴⁵ Nd	1.26	41(11)	5.76	0.91E+05(0.14E+05)	0.58(2)
¹⁴⁶ Nd	1.92	50(10)	7.57	0.53E+06(0.61E+05)	0.61(2)
¹⁴⁷ Nd	0.84	37(12)	5.29	0.15E+06(0.23E+05)	0.54(2)
¹⁴⁸ Nd	1.14	17(7)	7.33	0.21E+07(0.85E+06)	0.53(3)
¹⁴⁹ Nd	0.24	44(13)	5.04	0.29E+06(0.46E+05)	0.55(2)
¹⁵¹ Nd	0.60	50(14)	5.34	0.29E+06(0.43E+05)	0.55(2)
¹⁴⁸ Pm	0.48	71(17)	5.89	0.16E+07(0.44E+06)	0.54(2)
¹⁴⁸ Sm	1.62	22(4)	8.14	0.16E+07(0.18E+06)	0.58(1)
¹⁵⁰ Sm	2.04	79(18)	7.99	0.37E+07(0.52E+06)	0.55(1)
¹⁵¹ Sm	0.36	92(20)	5.60	0.75E+06(0.13E+06)	0.58(2)
¹⁵² Sm	1.14	31(9)	8.26	0.73E+07(0.12E+07)	0.58(2)
¹⁵³ Sm	0.30	68(14)	5.87	0.88E+06(0.31E+06)	0.59(3)
¹⁵⁵ Sm	0.24	25(10)	5.81	0.41E+06(0.57E+05)	0.57(3)
¹⁵² Eu	0.24	307(36)	6.31	0.12E+08(0.17E+07)	0.57(1)
¹⁵³ Eu	0.42	47(11)	8.55	0.36E+08(0.29E+07)	0.60(1)
¹⁵⁴ Eu	0.36	296(35)	6.44	0.88E+07(0.15E+07)	0.59(1)

¹⁵⁵ Eu	0.90	54(12)	8.15	0.12E+08(0.28E+07)	0.59(2)
¹⁵⁶ Eu	0.24	78(18)	6.34	0.24E+07(0.28E+06)	0.59(2)
¹⁵³ Gd	0.24	75(18)	6.25	0.36E+07(0.60E+06)	0.56(2)
¹⁵⁵ Gd	0.36	78(18)	6.44	0.36E+07(0.50E+06)	0.57(1)
¹⁵⁶ Gd	1.62	59(8)	8.54	0.10E+08(0.16E+07)	0.57(1)
¹⁵⁷ Gd	0.72	109(21)	6.36	0.13E+07(0.19E+06)	0.60(2)
¹⁵⁸ Gd	1.26	38(10)	7.94	0.32E+07(0.40E+06)	0.59(2)
¹⁵⁹ Gd	0.72	66(17)	5.94	0.64E+06(0.70E+05)	0.57(2)
¹⁶¹ Gd	0.36	25(10)	5.64	0.27E+06(0.38E+05)	0.57(3)
¹⁶⁰ Tb	0.36	78(19)	6.26	0.46E+07(0.20E+07)	0.54(2)
¹⁵⁹ Dy	0.48	56(15)	6.83	0.20E+07(0.44E+06)	0.61(2)
¹⁶¹ Dy	0.60	78(18)	6.45	0.21E+07(0.25E+06)	0.57(1)
¹⁶² Dy	1.98	128(19)	8.20	0.60E+07(0.36E+07)	0.58(3)
¹⁶³ Dy	0.36	53(15)	6.27	0.90E+06(0.15E+06)	0.61(2)
¹⁶⁴ Dy	0.96	20(10)	7.66	0.23E+07(0.42E+06)	0.58(3)
¹⁶⁵ Dy	0.60	54(15)	5.72	0.33E+06(0.59E+05)	0.59(2)
¹⁶⁶ Ho	0.48	112(22)	6.24	0.38E+07(0.75E+06)	0.55(2)
¹⁶³ Er	0.36	49(14)	6.90	0.76E+07(0.13E+07)	0.55(2)
¹⁶⁵ Er	0.48	71(17)	6.65	0.26E+07(0.43E+06)	0.59(2)
¹⁶⁷ Er	0.84	87(19)	6.44	0.14E+07(0.20E+06)	0.58(2)
¹⁶⁸ Er	1.32	49(15)	7.77	0.34E+07(0.61E+06)	0.58(2)
¹⁶⁹ Er	0.60	30(9)	6.00	0.63E+06(0.92E+05)	0.54(2)
¹⁷¹ Er	0.36	33(12)	5.68	0.39E+06(0.55E+05)	0.57(2)
¹⁷⁰ Tm	0.72	154(25)	6.59	0.56E+07(0.11E+07)	0.56(1)
¹⁶⁹ Yb	0.84	75(18)	6.87	0.28E+07(0.32E+06)	0.57(1)
¹⁷¹ Yb	0.96	83(19)	6.62	0.27E+07(0.45E+06)	0.54(1)
¹⁷² Yb	1.68	89(14)	8.02	0.57E+07(0.74E+06)	0.57(1)
¹⁷³ Yb	0.54	35(10)	6.37	0.99E+06(0.11E+06)	0.57(2)
¹⁷⁴ Yb	1.74	63(13)	7.46	0.16E+07(0.22E+06)	0.57(1)
¹⁷⁵ Yb	1.08	62(16)	5.82	0.38E+06(0.56E+05)	0.55(2)
¹⁷⁷ Yb	0.30	19(7)	5.57	0.33E+06(0.48E+05)	0.54(2)
¹⁷⁶ Lu	0.72	156(25)	6.29	0.51E+07(0.82E+06)	0.54(1)
¹⁷⁷ Lu	0.72	41(13)	7.07	0.80E+07(0.12E+07)	0.52(2)
¹⁷⁵ Hf	0.30	39(10)	6.71	0.41E+07(0.86E+06)	0.55(2)
¹⁷⁷ Hf	0.54	43(11)	6.38	0.20E+07(0.48E+06)	0.54(2)
¹⁷⁸ Hf	1.56	87(19)	7.63	0.44E+07(0.64E+06)	0.56(1)
¹⁷⁹ Hf	0.54	36(10)	6.10	0.12E+07(0.21E+06)	0.53(2)
¹⁸⁰ Hf	1.26	53(12)	7.39	0.25E+07(0.31E+06)	0.57(1)
¹⁸¹ Hf	0.24	20(9)	5.70	0.62E+06(0.26E+06)	0.53(3)
¹⁸¹ Ta	0.24	17(9)	7.58	0.11E+08(0.96E+06)	0.55(2)
¹⁸² Ta	0.48	85(19)	6.06	0.25E+07(0.26E+06)	0.54(1)
¹⁸³ Ta	0.48	17(8)	6.93	0.33E+07(0.69E+06)	0.53(2)
¹⁸¹ W	0.48	49(14)	6.68	0.37E+07(0.91E+06)	0.55(2)
¹⁸³ W	0.42	28(9)	6.19	0.13E+07(0.34E+06)	0.54(2)
¹⁸⁴ W	1.32	46(14)	7.41	0.29E+07(0.37E+06)	0.55(2)
¹⁸⁵ W	0.24	25(11)	5.75	0.74E+06(0.10E+06)	0.54(2)
¹⁸⁷ W	0.24	25(10)	5.47	0.51E+06(0.62E+05)	0.53(2)
¹⁸⁶ Re	0.36	71(17)	6.18	0.41E+07(0.51E+06)	0.53(1)
¹⁸⁸ Re	0.24	73(17)	5.87	0.38E+07(0.54E+06)	0.52(1)
¹⁸⁷ Os	0.42	47(11)	6.29	0.23E+07(0.50E+06)	0.54(2)
¹⁸⁸ Os	1.86	68(13)	7.99	0.83E+07(0.89E+06)	0.52(1)
¹⁸⁹ Os	0.60	62(16)	5.92	0.17E+07(0.18E+06)	0.52(1)
¹⁹⁰ Os	1.98	85(15)	7.79	0.58E+07(0.64E+06)	0.52(1)
¹⁹¹ Os	0.36	58(15)	5.76	0.95E+06(0.12E+06)	0.56(2)
¹⁹³ Os	0.36	20(9)	5.58	0.58E+06(0.76E+05)	0.51(2)
¹⁹² Ir	0.24	141(24)	6.21	0.59E+07(0.77E+06)	0.56(1)
¹⁹³ Ir	0.48	41(14)	7.76	0.19E+08(0.34E+07)	0.56(2)
¹⁹⁴ Ir	0.24	78(18)	6.07	0.25E+07(0.35E+06)	0.56(2)
¹⁹⁵ Pt	0.48	54(15)	6.11	0.29E+06(0.96E+05)	0.66(3)
¹⁹⁶ Pt	1.92	75(18)	7.92	0.21E+07(0.41E+06)	0.59(2)

¹⁹⁷ Pt	0.48	37(12)	5.85	0.18E+06(0.51E+05)	0.63(3)
¹⁹⁸ Au	0.42	65(13)	6.51	0.13E+07(0.12E+06)	0.62(1)
²⁰⁰ Hg	1.86	43(8)	8.03	0.47E+06(0.11E+06)	0.66(2)
²⁰¹ Hg	0.48	25(10)	6.23	0.56E+05(0.70E+04)	0.75(4)
²⁰² Hg	1.74	41(11)	7.76	0.18E+06(0.38E+05)	0.72(3)
²⁰³ Hg	0.66	15(6)	5.93	0.29E+05(0.15E+05)	0.70(6)
²⁰⁴ Tl	0.36	29(11)	6.66	0.11E+06(0.19E+05)	0.76(4)
²⁰⁶ Tl	1.02	15(4)	6.50	0.10E+05(0.40E+04)	0.84(6)
²⁰⁵ Pb	1.68	44(13)	6.73	0.29E+05(0.70E+04)	0.78(5)
²⁰⁷ Pb	0.72	4(3)	6.74	0.33E+04(0.63E+03)	0.91(10)
²⁰⁸ Pb	3.42	26(8)	7.37	0.21E+04(0.68E+03)	0.91(9)
²⁰⁹ Pb	1.08	5(3)	3.94	0.18E+03(0.78E+02)	0.78(19)
²¹⁰ Bi	0.42	24(8)	4.61	0.23E+04(0.33E+03)	0.92(7)
²²⁷ Ra	0.30	52(12)	4.56	0.15E+07(0.35E+06)	0.42(1)
²³⁰ Th	0.96	44(13)	6.79	0.31E+08(0.13E+08)	0.43(2)
²³¹ Th	0.24	59(15)	5.12	0.81E+07(0.14E+07)	0.41(1)
²³³ Th	0.36	75(18)	4.79	0.40E+07(0.13E+07)	0.41(2)
²³⁵ Pa	0.24	20(9)	6.09	0.12E+09(0.21E+08)	0.38(1)
²³³ U	0.36	54(15)	5.74	0.18E+08(0.33E+07)	0.42(1)
²³⁴ U	1.08	78(18)	6.84	0.31E+08(0.69E+07)	0.45(1)
²³⁵ U	0.30	59(13)	5.30	0.76E+07(0.37E+07)	0.43(2)
²³⁶ U	1.08	92(20)	6.55	0.32E+08(0.83E+07)	0.43(1)
²³⁷ U	0.60	79(18)	5.13	0.52E+07(0.61E+06)	0.41(1)
²³⁸ U	1.08	71(17)	6.15	0.12E+08(0.29E+07)	0.42(1)
²³⁹ U	0.84	75(18)	4.81	0.38E+07(0.52E+06)	0.37(1)
²³⁸ Np	0.24	82(18)	5.49	0.32E+08(0.29E+07)	0.41(1)
²³⁹ Pu	0.42	49(11)	5.65	0.94E+07(0.12E+07)	0.43(1)
²⁴⁰ Pu	1.08	58(15)	6.53	0.19E+08(0.20E+07)	0.43(1)
²⁴¹ Pu	0.30	46(11)	5.24	0.60E+07(0.62E+06)	0.42(1)
²⁴² Pu	1.08	44(13)	6.31	0.17E+08(0.25E+07)	0.41(1)
²⁴³ Pu	0.30	26(8)	5.03	0.46E+07(0.72E+06)	0.39(1)
²⁴² Am	0.24	65(16)	5.54	0.33E+08(0.72E+07)	0.40(1)
²⁴³ Am	0.30	38(10)	6.36	0.77E+08(0.21E+08)	0.42(1)
²⁴⁴ Am	0.36	106(20)	5.37	0.27E+08(0.52E+07)	0.40(1)
²⁴³ Cm	0.84	32(11)	5.70	0.67E+07(0.16E+07)	0.40(1)
²⁴⁴ Cm	1.08	32(11)	6.80	0.20E+08(0.31E+07)	0.43(1)
²⁴⁵ Cm	0.48	58(15)	5.52	0.71E+07(0.92E+06)	0.43(1)
²⁴⁶ Cm	1.02	36(10)	6.46	0.23E+08(0.10E+08)	0.41(2)
²⁴⁷ Cm	0.36	61(16)	5.16	0.26E+07(0.48E+06)	0.45(1)
²⁴⁸ Cm	1.08	32(11)	6.21	0.82E+07(0.19E+07)	0.41(1)
²⁴⁹ Cm	0.24	32(14)	4.71	0.25E+07(0.44E+06)	0.40(2)
²⁵⁰ Bk	0.24	97(20)	4.97	0.13E+08(0.17E+07)	0.40(1)
²⁵⁰ Cf	1.08	38(8)	6.62	0.17E+08(0.27E+07)	0.43(1)
²⁵³ Cf	0.24	12(7)	4.81	0.31E+07(0.55E+06)	0.37(2)

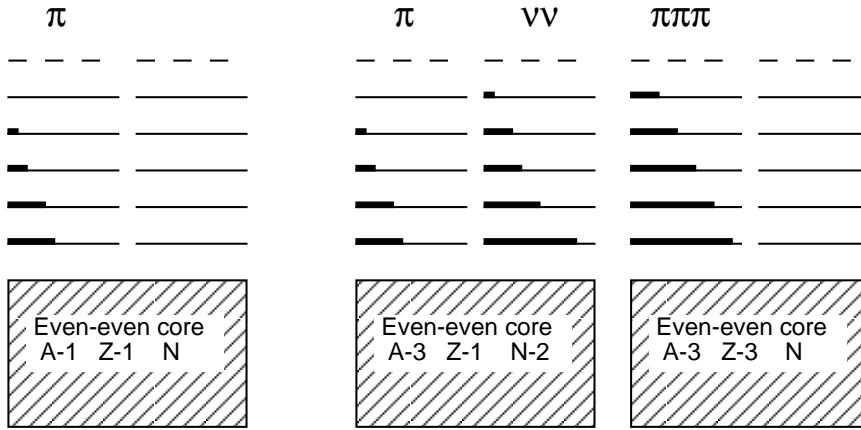


FIG. 1. Illustration of thermal excitations in an odd proton nucleus, where the horizontal bars indicate how much the orbitals are filled on the average. In the case of no broken pairs (left diagram), the single proton has maximum number of quantum states (multiplicity) available. The three quasiparticle excitation has to include either a $\pi\nu^2$ or a π^3 configuration (two right diagrams). Here, the Pauli blocking reduces the multiplicity and gives a lower quasiparticle entropy.

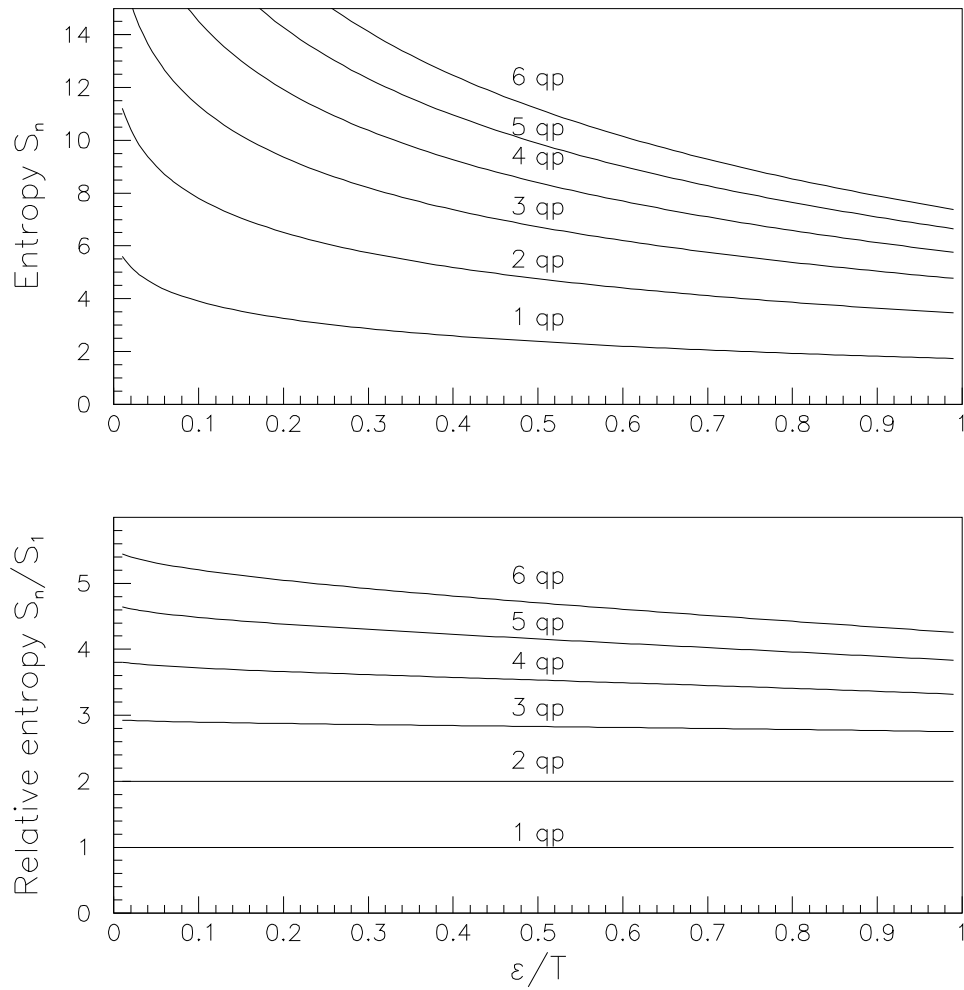


FIG. 2. The entropy S_n of n quasiparticles. The entropy increases with increasing temperature T for fixed level spacing ϵ . The lower part demonstrates that the Pauli blocking reduces the entropy per quasiparticle for $n > 2$.

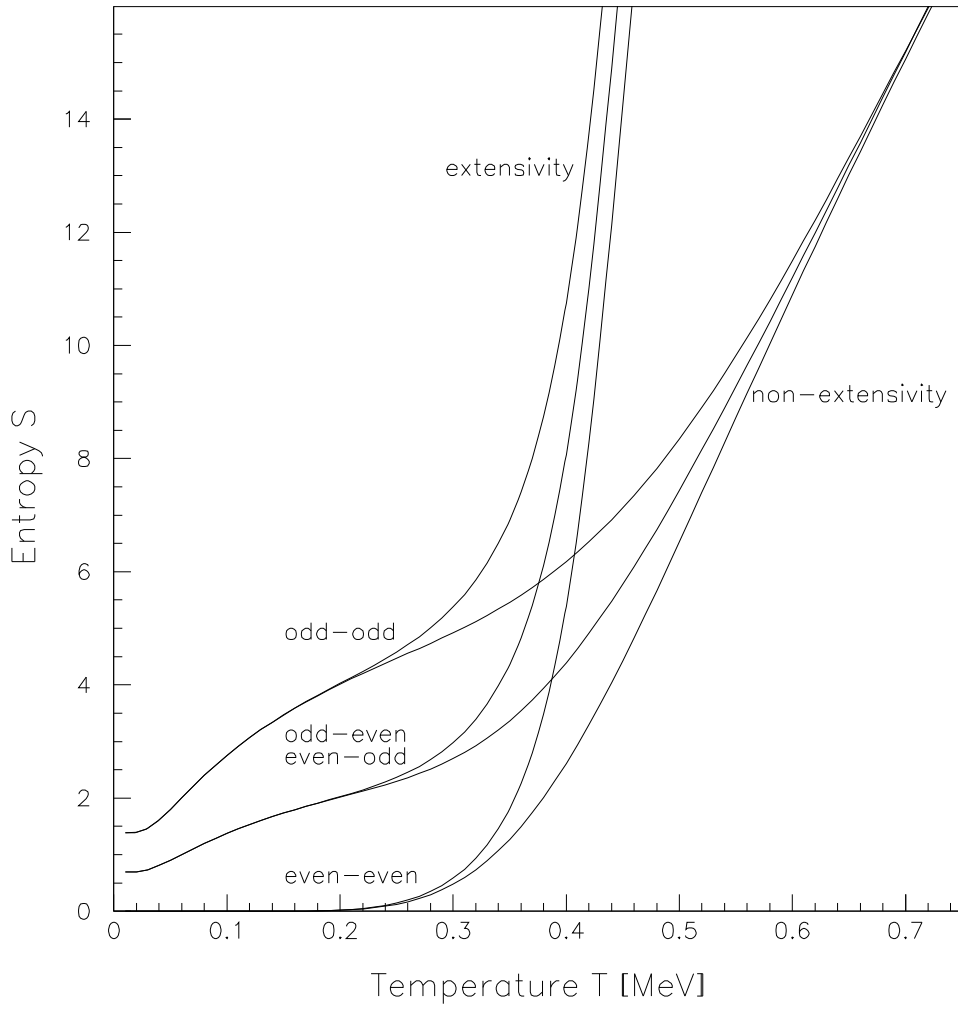


FIG. 3. The total entropy calculated for even-even, odd-mass and odd-odd nuclei allowing a maximum of five broken pairs. The extensive and non-extensive calculations are performed with Eqs. (18) and (17), respectively. The parameters used are $\Delta = 0.9$ MeV and $\epsilon = 0.15$ MeV.

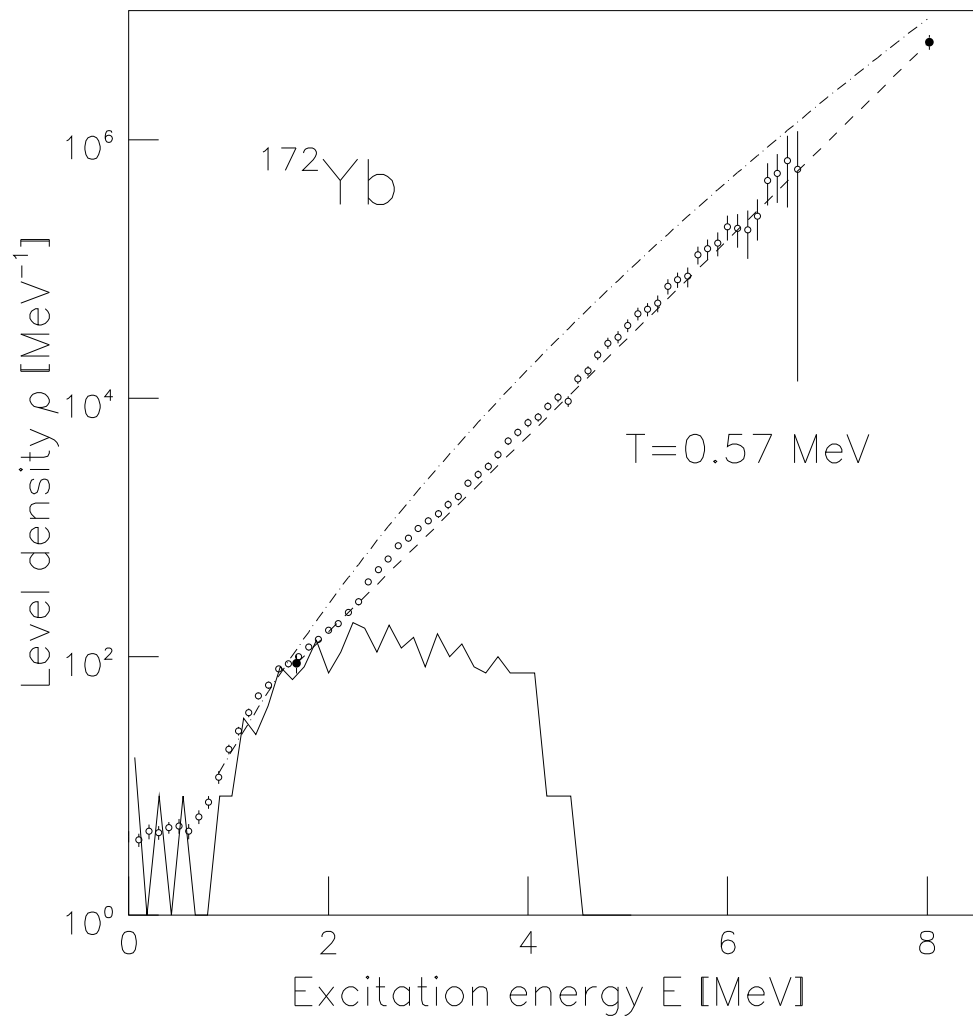


FIG. 4. Level densities in ^{172}Yb , showing the two anchor points (filled circles). The solid line is based on the counting of discrete known levels. Also shown are the backshifted level density prediction of Egidy et al. [9] (dashed-dotted) and the constant temperature formula (dashed).

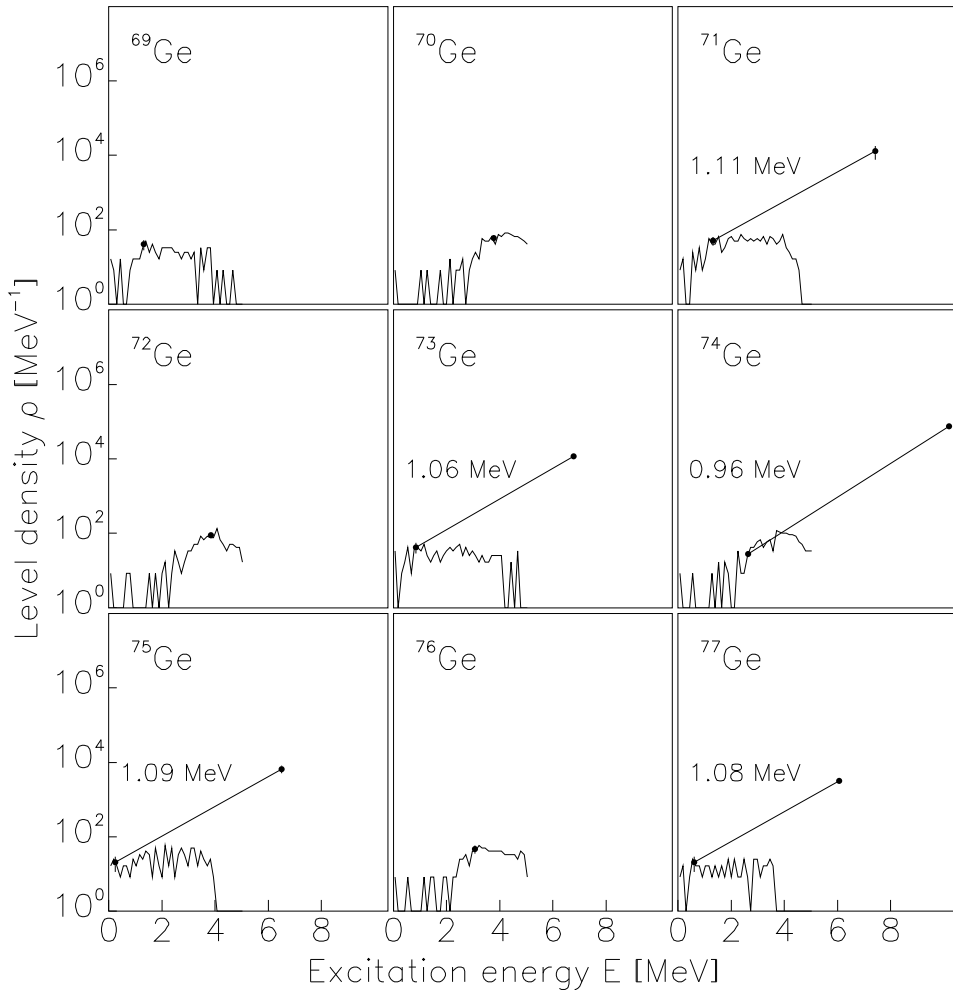


FIG. 5. The level density anchor points extracted for $^{69-77}\text{Ge}$. The lower point is based on known discrete levels. In cases where the second anchor point is known, the extracted temperature T is quoted.

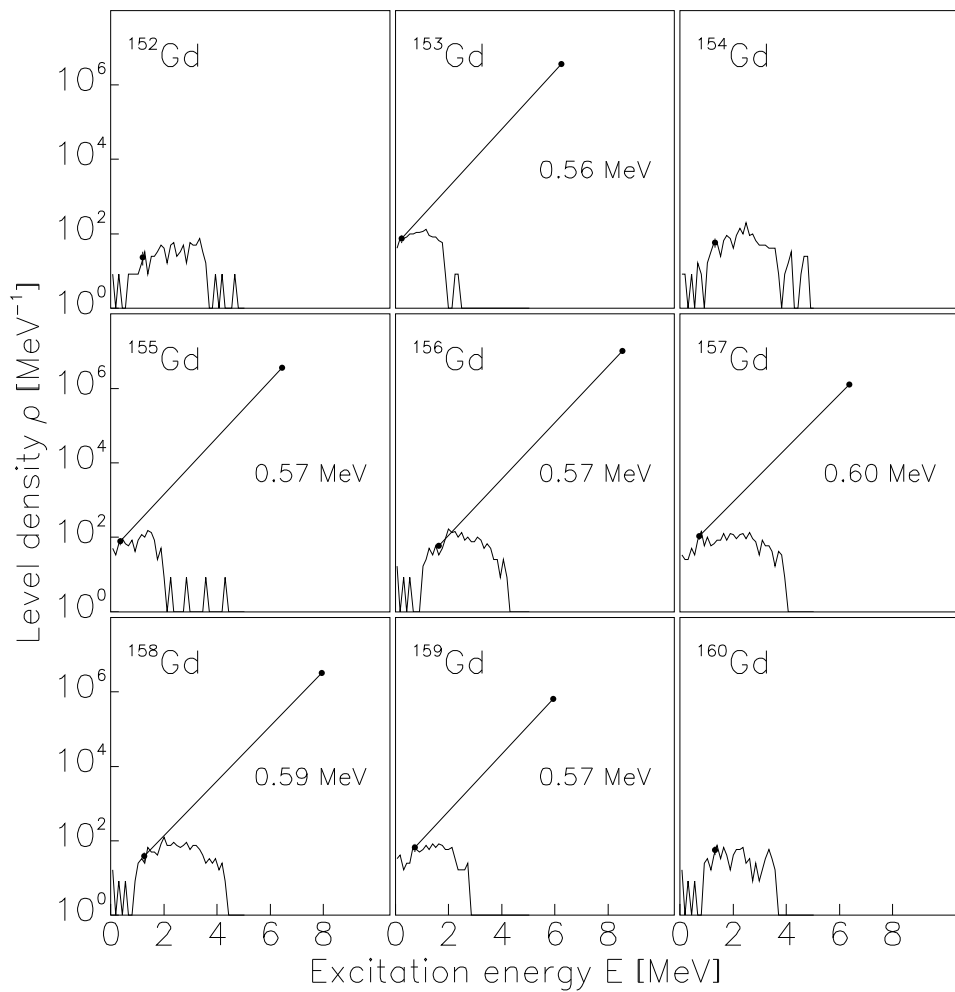


FIG. 6. Anchor points for $^{152-160}\text{Gd}$, see text of Fig. 5.

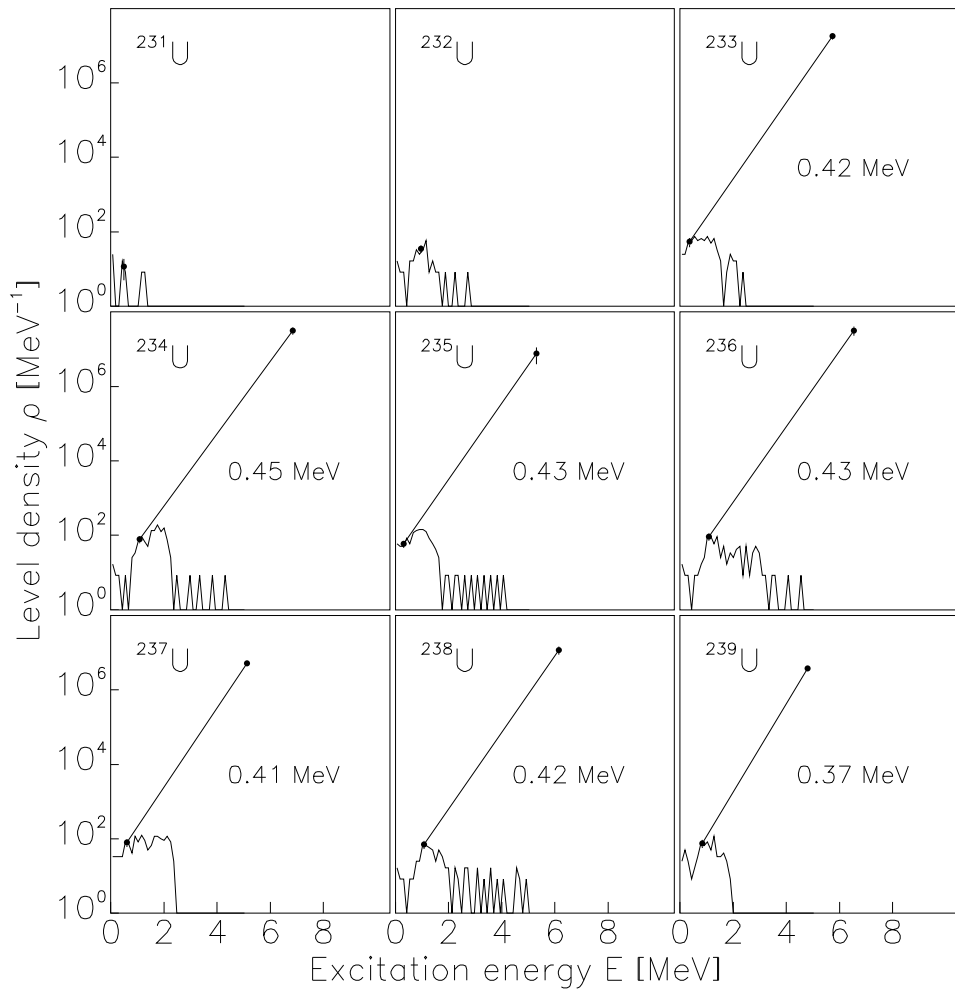


FIG. 7. Anchor points for $^{231-239}\text{U}$, see text of Fig. 5.

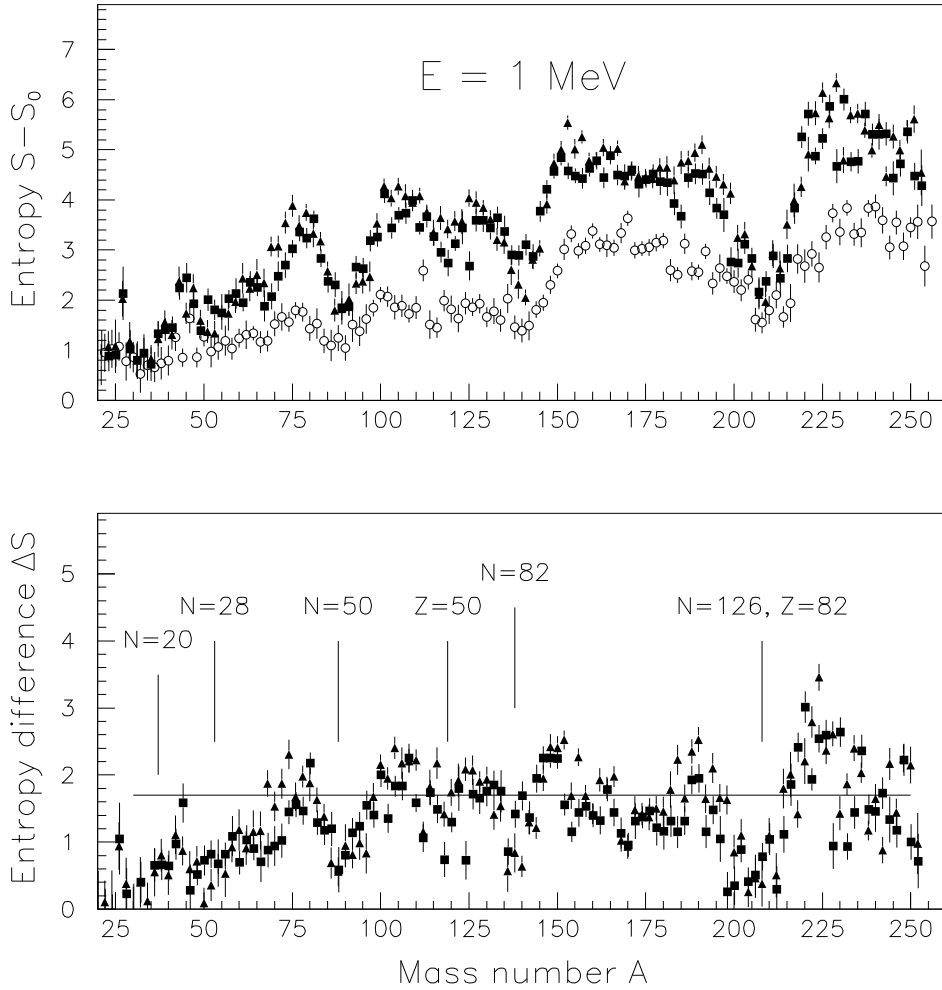


FIG. 8. Entropy as function of mass number at 1 MeV of excitation energy. The upper panel shows that the odd-even (filled triangles) and even-odd (filled squares) nuclei exhibit higher entropy than the even-even (open circles) nuclei. In the lower panel, the entropy difference between odd-mass and even-even nuclei is shown, giving an average of $\Delta S \sim 1.7$ (solid line) for mid-shell nuclei. The approximate locations of the neutron and proton magic numbers are indicated. The data are based on the anchor points discussed in the text, and each data point is typically the average of 2-4 nuclei centered around the β -stability line.

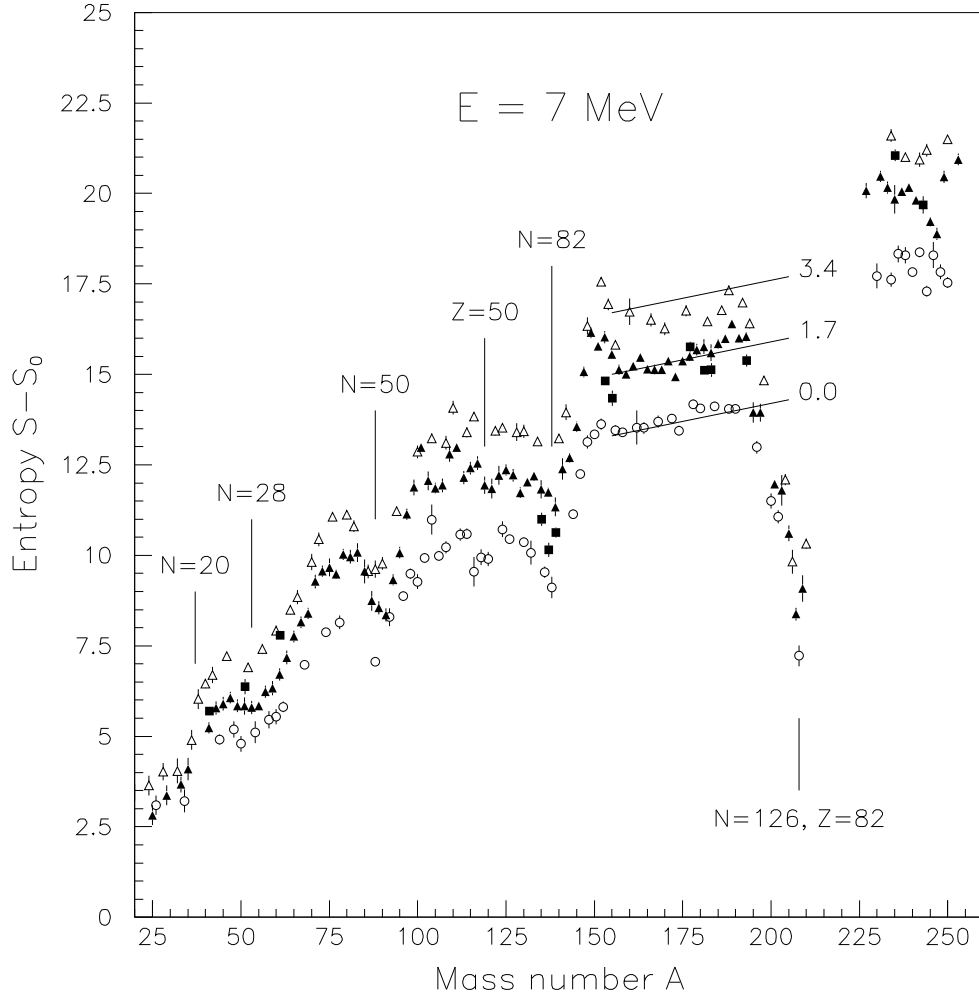


FIG. 9. Entropy as function of mass number at 7 MeV of excitation energy. The data are plotted for odd-odd (open triangles), odd-even (filled triangles), even-odd (filled squares) and even-even (open circles) nuclei, see text of Fig. 8. The three lines are drawn to indicate the entropy gaps between even-even, odd-mass and odd-odd nuclei.

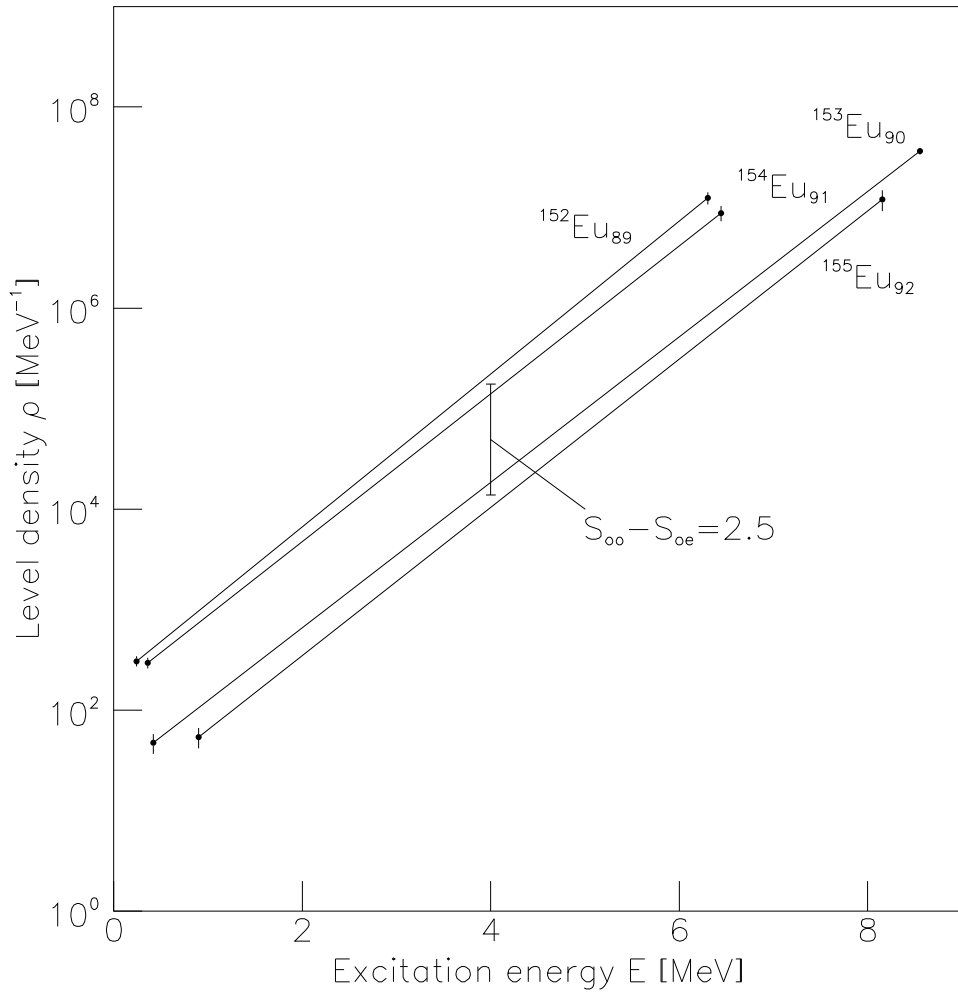


FIG. 10. Level densities and entropy difference for odd-even $^{153,155}\text{Eu}$ and odd-odd $^{152,154}\text{Eu}$ nuclei.

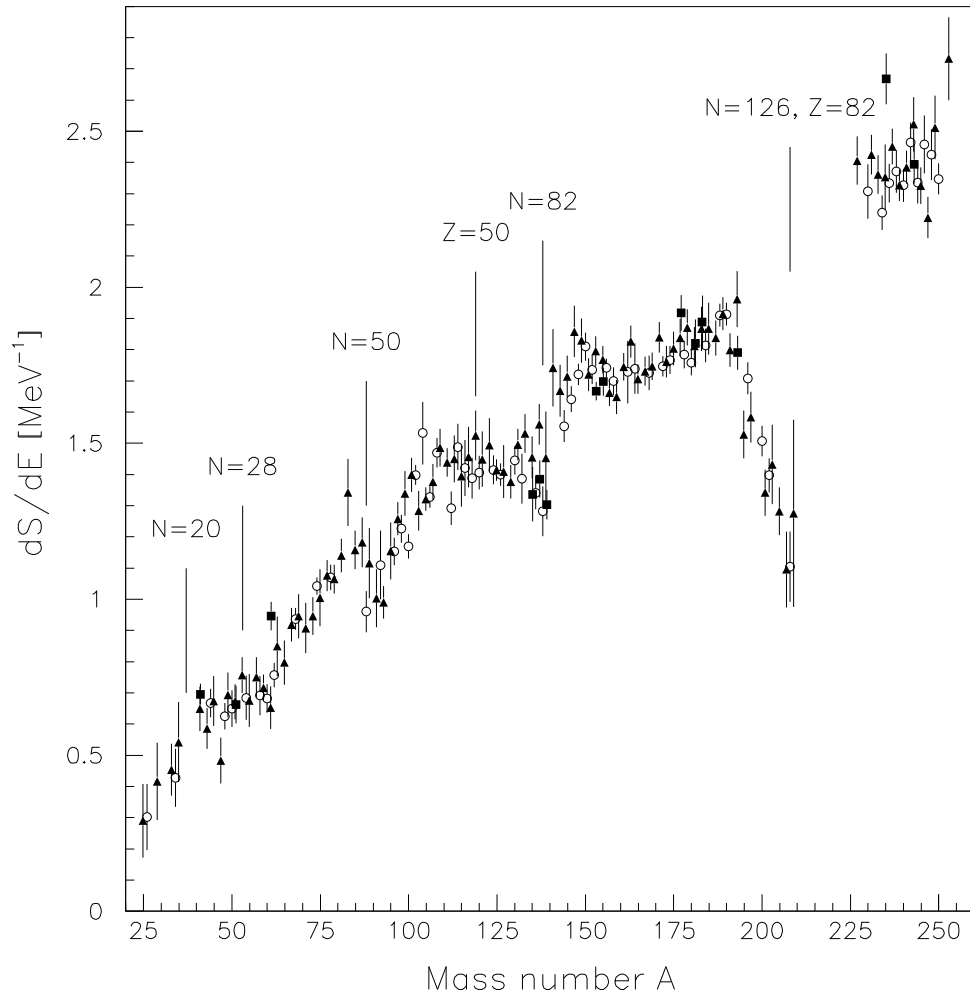


FIG. 11. The derivative of entropy with respect to excitation energy as function of mass number. The derivatives are determined from the anchor points of nuclei along the line of β -stability. The data are plotted for odd-even (filled triangles), even-odd (filled squares) and even-even (open circles) nuclei.

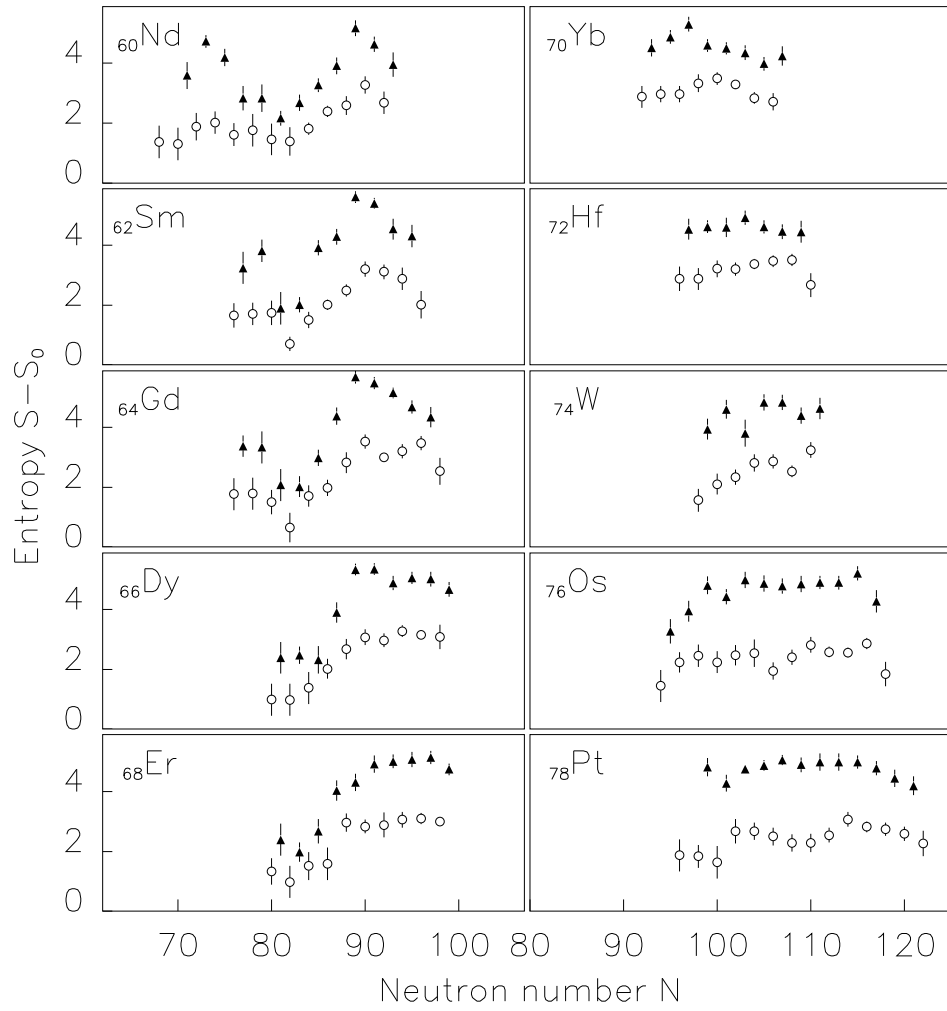


FIG. 12. The entropies extracted at 1 MeV of excitation energy for odd-even (filled triangles) and even-even (open circles) rare earth isotopes. The data demonstrates that the entropy difference ΔS between odd-even and even-even isotopes is strongly reduced at the $N = 82$ shell closure.

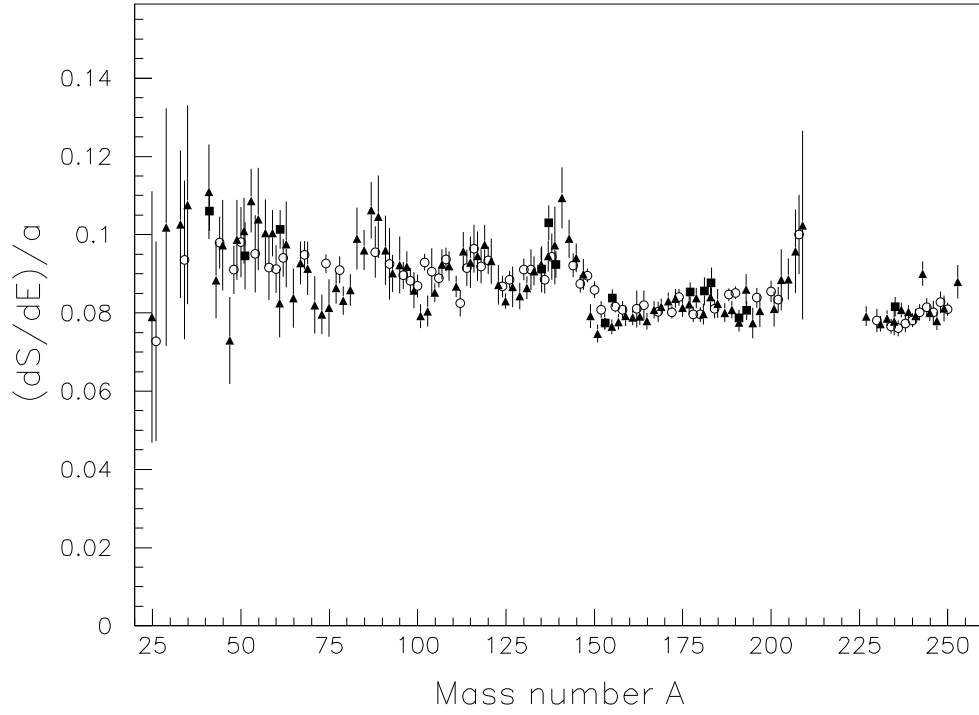


FIG. 13. The experimentally available quantity $(\partial S/\partial E)/a$ is proportional to ϵ/T , which determines the single quasiparticle entropy in our model.

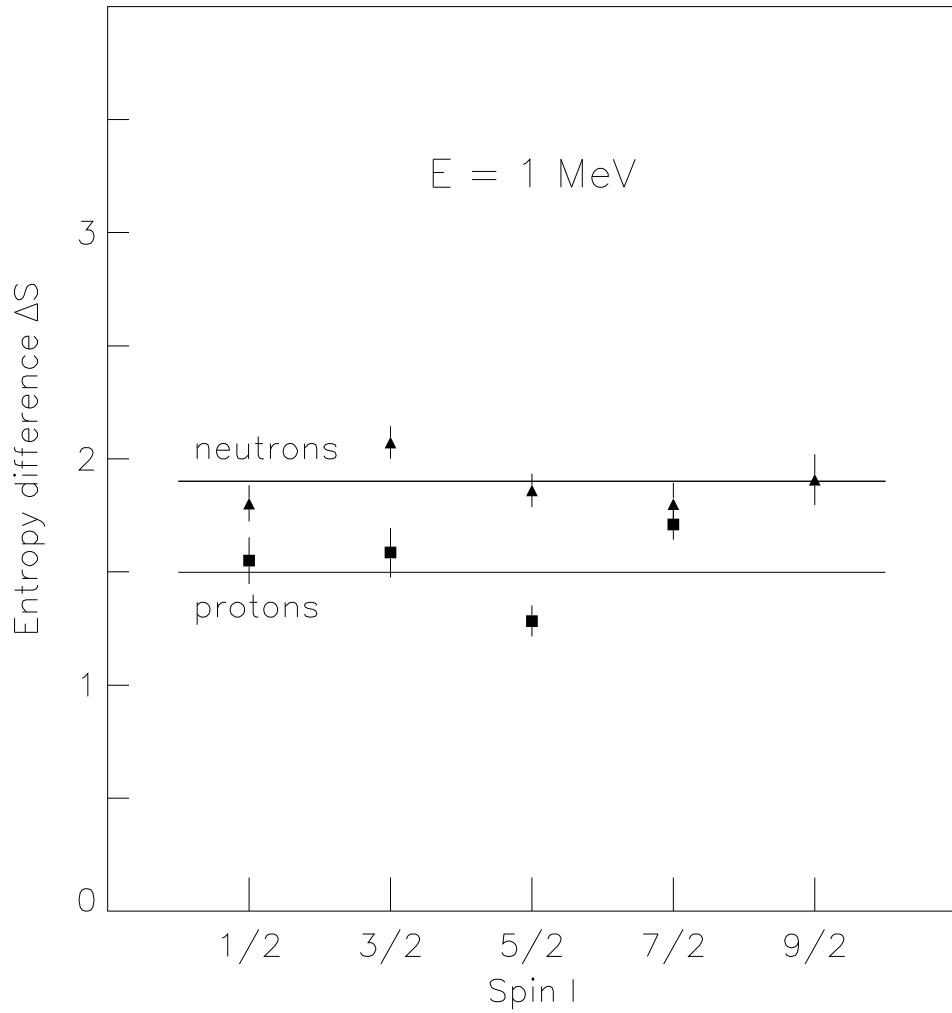


FIG. 14. The entropy difference ΔS for odd-even (filled triangles) and even-odd (filled squares) nuclei relative to even-even nuclei as function of ground state spin. The data are taken for nuclei with $Z = 60 - 78$ and $N = 90 - 110$. The solid lines are the averages for protons (1.5) and neutrons (1.9).

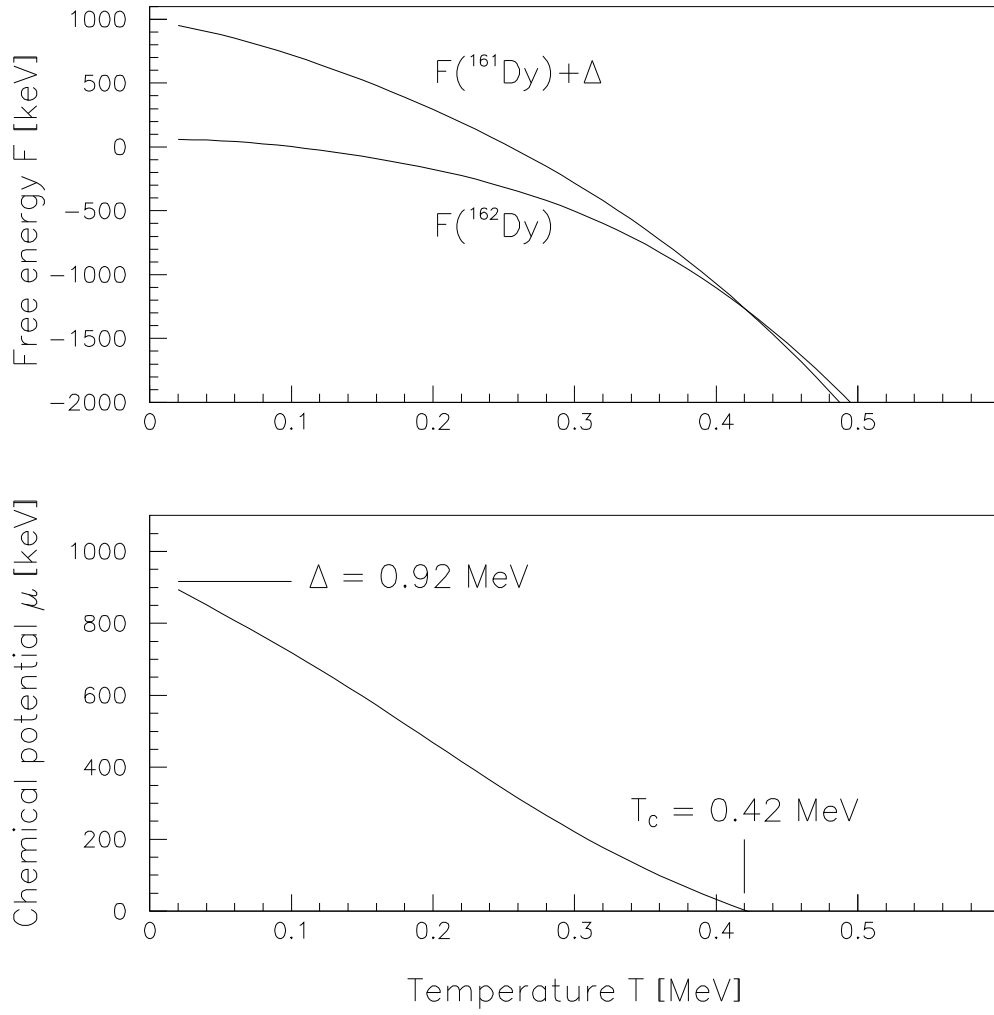


FIG. 15. The experimentally deduced Helmholtz free energy for $^{161,162}\text{Dy}$ extracted in the canonical ensemble. The critical temperature for the quenching of pair correlations is found at $T_c = 0.42$ MeV, where the chemical potential is $\mu \sim 0$.